Symmetry **2011**, *3*, 699-749; doi:10.3390/sym3040699

OPEN ACCESS

symmetry

ISSN 2073-8994

www.mdpi.com/journal/symmetry

Article

d-Wave Superconductivity and s-Wave Charge Density Waves: Coexistence between Order Parameters of Different Origin and Symmetry

Toshikazu Ekino [1], Alexander M. Gabovich [2,⋆], Mai Suan Li [3], Marek Pękała [4], Henryk Szymczak [3] and Alexander I. Voitenko [2]

[1] Hiroshima University, Graduate School of Integrated Arts and Sciences, Higashi-Hiroshima 739-8521, Japan; E-Mail: ekino@hiroshima-u.ac.jp

[2] Institute of Physics, National Academy of Sciences of Ukraine, 46, Nauka Ave., Kyiv 03680, Ukraine; E-Mail: voitenko@iop.kiev.ua

[3] Institute of Physics, Al. Lotników 32/46, Warsaw PL-02-668, Poland; E-Mails: masli@ifpan.edu.pl (M.S.L.); szymh@ifpan.edu.pl (H.S.)

[4] Department of Chemistry, University of Warsaw, Al. Zwirki i Wigury 101, Warsaw PL-02-089, Poland; E-Mail: pekala@chem.uw.edu.pl

⋆ Author to whom correspondence should be addressed; E-Mail: gabovich@iop.kiev.ua; Tel.: +38-044-525-0820; Fax: +38-044-525-1589.

Received: 26 May 2011; in revised form: 8 October 2011 / Accepted: 11 October 2011 / Published: 20 October 2011

Abstract: A review of the theory describing the coexistence between d-wave superconductivity and s-wave charge-density-waves (CDWs) is presented. The CDW gapping is identified with pseudogapping observed in high-T_c oxides. According to the cuprate specificity, the analysis is carried out for the two-dimensional geometry of the Fermi surface (FS). Phase diagrams on the $\sigma_0 - \alpha$ plane—here, σ_0 is the ratio between the energy gaps in the parent pure CDW and superconducting states, and the quantity 2α is connected with the degree of dielectric (CDW) FS gapping—were obtained for various possible configurations of the order parameters in the momentum space. Relevant tunnel and photoemission experimental data for high-T_c oxides are compared with theoretical predictions. A brief review of the results obtained earlier for the coexistence between s-wave superconductivity and CDWs is also given.

Keywords: order parameter symmetry; superconductivity; charge-density waves; phase diagrams

Classification: PACS 74.20.-z; 74.20.Rp; 71.45.Lr; 74.72.-h

1. Introduction

Superconductivity in high-T_c oxides has been for a long time suspected to exhibit non-conventional order parameter symmetry [1]. Nevertheless, there is no consensus that it is really the case. Indeed, some phase-sensitive experiments show isotropic s-wave superconductivity (SC) [2–5], whereas the majority of measurements reveal $d_{x^2-y^2}$-wave Cooper pairing [6–15] or, may be, an extended d-wave gap with higher angle harmonics [16]. Moreover, a lot of phase-insensitive evidence can be regarded as a manifestation of the extended s-wave pairing [17–22]. (To reconcile the latter interpretation with the observed d-wave-like data [6–8,11,13], the author of Reference [17] supposed that the d-wave symmetry is inherent to "the degraded surfaces" rather than to the samples' bulk.) It should also be emphasized that various power-law bulk temperature, T, dependences cannot be regarded as a ponderable argument for the existence of nodes on the Fermi surface (FS), which are appropriate to non-conventional superconducting order parameters [23,24]. Namely, a disordered multidomain structure of high-T_c oxides might be the origin of the transformation of Bardeen–Copper–Schrieffer (BCS) exponential dependences for a number of gap-related properties into power-law ones due to the averaging over those domains with varying T_c's and corresponding energy gaps [25–29]. The treatment of high-T_c superconductors as spatially inhomogeneous percolating conglomerates was earlier suggested in Reference [30] from other considerations (see also References [31–34]).

Note, that for thermodynamic properties, governed by energy gaps, the sign, as well as the phase, of superconducting order parameter is irrelevant, at least in the standard situation, when the actual order parameter is not a superposition of terms with different symmetries, the possibility, which can not been ruled out [35,36]. On the other hand, the existence and character of nodes matter (see a thorough account in References [23,24]), making the electron spectrum gapless and the T-dependences power-law ones, as was indicated above.

The picture becomes richer, if superconductivity coexists with another long-range order, e.g., ferromagnetism or antiferromagnetism [37–48], spin-density waves (SDWs) [49–56] or charge-density waves (CDWs) [46,50–53,56–60]. In particular, following the seminal work [61] (see also Reference [62] based on the specific two-dimensional tight-binding model with first- and second-neighbor couplings taken into consideration), we have developed a theory of CDW superconductors for the s-wave superconducting order parameter [63–73]. In agreement with the statement made above, the thermodynamics does not depend on the phases of both order parameters, whereas quasiparticle and Josephson currents do [74–86]. There are a good many CDW superconductors, for which the model [61,71] is suitable (see, e.g., References [46,52,60,87–92]).

Therefore, we suggested a model of CDW superconductors with $d_{x^2-y^2}$-symmetry on the basis of the electron spectrum peculiarities found in numerous experiments for high-T_c oxides [93–101]. Their enigmatic properties are treated below in the framework of this model. Most likely, the actual truth for the materials concerned lies in between the ultimate cases of s-wave and d-wave CDW

superconductors (see, e.g., Reference [102]). The main problem of our approach justification is to prove the CDW existence in cuprates, which, fortunately, has already been done by scanning tunnel microscopy (STM), photoemission (ARPES) and other studies. Talking about the "ultimate proof", a concept not directly applicable to the extremely involved phenomena in solid state physics [103], one should not expect [104] for a simple model to be verified or falsified in the Popper's spirit [105]. We can yet show the soundness of our scenario and its fruitful corollaries. By doing this we rely not only on direct observations of CDWs in the real **r**-space but also on the identification of mysterious pseudogaps (the energy gaps of a still ambiguous nature both below and above the critical temperature, T_c) often observed in high-T_c ceramics [100,101,106–112] with the CDW gaps. We emphasize that the observed coherent long-range phenomena occur against a non-homogeneous background of the intrinsically non-stoichiometric materials [113–118].

This review of our theory, partially published elsewhere [60,119–121], and related problems deals with cuprates but it can also be applied to other superconductors with unstable electron spectrum and non-conventional order parameter symmetry. Hereafter, we adopt the already expressed viewpoint that pseudogaps in cuprates are CDW gaps, although other interpretations are respected and mentioned in some places. Anyway, experimental data are presented without prejudices.

The outline of the article is as follows. The evidence about CDW and pseudogap manifestations in cuprates is presented in Section 2. The theoretical formulation is given in Sections 3–5. Sections 6–11 contains analytical and numerical results of calculations, as well as the detailed discussion. Conclusions are made in Section 12.

2. CDW and Pseudogap Evidence in Cuprates

Ion displacements—called periodic lattice distortions (PLDs)—accompanied by electron density modulations (CDWs) [122,123] were observed in almost all high-T_c oxides using various direct techniques [50–52,56,60,124–126]. Among them one should differentiate between checkerboard superstructures [127–132] (these are quite natural for the electron distribution with four-fold rotational symmetry inherent to cuprates with their quasi-two-dimensional CuO_2 planes [93,133–136]) and distorted states with broken rotational symmetry, e.g., unidirectional CDWs [129,130,137–140] or more disordered nematic configurations [56,124,141–144]. If thin static or fluctuating charged domains alternate with spin-ordered ones, *i.e.*, a peculiar unidirectional phase separation occurs (more general phase separation scenarios were proposed long ago for versatile objects [145–147]), the electronic state of a crystal is frequently called a stripe phase [56,137,148–150]. One should also bear in mind the possibility of loop-current electron ordering [56,124,151], going back to states predicted for the excitonic insulator [152].

Checkerboard-like $4a_0 \times 4a_0$ (a_0 is a lattice constant) CDW states were found in $Ca_{2-x}Na_xCuO_2Cl_2$ by STM [153] and photoemission measurements [154]. Similar periodic patterns were observed in tunnel studies of $Bi_2Sr_2CaCu_2O_{8+\delta}$(BSCCO) [128,155–159], $Bi_2Sr_{2-x}La_xCuO_{6+\delta}$ [117], and $Bi_{2-y}Pb_ySr_{2-z}La_zCuO_{6+x}$ [97]. In $Bi_2Sr_{2-x}La_xCuO_{6+\delta}$ the existence of checkerboard structures was also shown in combined STM-ARPES investigations [160].

Unidirectional PLDs were observed in $La_{1.875}Ba_{0.125}CuO_4$ and $La_{1.875}Ba_{0.075}Sr_{0.05}CuO_4$ by neutron scattering [94], $La_{1.8-x}Eu_{0.2}Sr_xCuO_4$ by X-ray diffraction [161,162], $Ca_{1.88}Na_{0.12}CuO_2Cl_2$ and $Bi_2Sr_2Dy_{0.2}Ca_{0.8}Cu_2O_{8+\delta}$ by STM [140], $Bi_{2+x}Sr_{2-x}CuO_{6+\delta}$ by electron diffraction and high-resolution electron microscopy [163], $Bi_{2-x}Pb_xSr_2CaCu_2O_{8+y}$ by STM [164], and $Bi_2Sr_2CaCu_2O_{8+\delta}$ by X-ray diffraction [165,166]. It is crucial that CDWs were shown to exist both below and above T_c. We also emphasize that various kinds of modulations were found for the same material, BSCCO [128,155–159,165,166]. A transition from unidirectional to checkerboard CDWs may be stimulated, e.g., by doping, as in the case of $YBa_2Cu_3O_{7-\delta}$, where a Lifshits topological transition occurs at a hole concentration of 0.08 [167,168].

One should note that in the presence of impurities (for instance, an inevitably non-homogeneous distribution of oxygen atoms) the attribution of the observed charge order (if any) to unidirectional versus checkerboard type might be ambiguous [129]. Another remark must be made concerning commensurability of PLDs-CDWs. Namely, their wave vectors $\mathbf{Q}$ are, in general, incommensurate and doping-dependent [97,117], so that the expressions like $4a_0 \times 4a_0$ are always approximate, although correctly reflecting the four-fold symmetry of the distortions concerned.

Measurements of transport and photoemission properties in *non-superconducting* layered nickelates $R_{2-x}Sr_xNiO_4$ ($R = \mathrm{Nd}$, Eu), which are structurally similar to cuprates, revealed a correlation between the pseudogap emergence and charge ordering [169]. Pseudogaps appeared on the same Fermi surface (FS) sections as in cuprates, thus testifying the similarity between two classes of materials. Layered dichalcogenides constitute another group of materials with CDWs [122,123,170] similar to those in cuprates, as has been recently shown [171–174] (see also Reference [175]). In particular, a *true pseudogap*—a non-mean-field fluctuation precursor phenomenon [176–178]—is observed in 2*H*-$TaSe_2$ above the normal metal-incommensurate CDW transition temperature $T_{N-IC} \approx 122$ K [171]. Such a behavior comprises a strong argument in favor of the CDW nature of pseudogapping in cuprates as well.

As for pseudogaps, they were found in cuprates both above and below T_c, which is one of their most important features. The pseudogap is a depletion of the electron densities of states (DOS). It is natural that tunnel and ARPES experiments, which are very sensitive to DOS variations, made the largest contribution to the cuprate pseudogap data bank (see also references in our works [50–52,84–86]). Recent results show that the concept of two gaps (superconducting gap and pseudogap, the latter considered here as a CDW gap) [79,80,85,96,179–190] begins to dominate in the literature over the one-gap concept [191–201], according to which the pseudogap phenomenon is most frequently treated as a precursor of superconductivity (for instance, as properties of bipolaron gas above T_c that Bose-condenses below T_c [200]). The main arguments, which show that superconducting and pseudo- gaps are not identical, are the coexistence of both features below T_c [106,202], their different position in the momentum space of the two-dimensional Brillouin zone [187,203–206], and their differing behavior in the external magnetic fields $\mathbf{H}$ [207], for various dopings [202], and under the effects of disorder [206].

Sometimes, evidence for CDW ordering may be rather indirect, although the very appearance of the phase transition is beyond any doubt. In cuprates, T-anomalies in the nuclear quadrupole resonance transverse relaxation rate in $YBa_2Cu_3O_{7-\delta}$ are the best example of such a behavior [208,209].

Whatever the pseudogap nature, some unusual properties still remain puzzling in the pseudogap physics. For instance, it was found [188] that the pseudogap in $Bi(Pb)_2Sr_2Ca(Tb)Cu_2O_{8+\delta}$ revealed by ARPES is nonmonotonic in T. Such a behavior, as they indicated, might be related to the existence of commensurate and incommensurate CDW gaps in a close analogy with the case of dichalcogenides [210]. Moreover, photoemission studies of $La_{1.875}Ba_{0.125}CuO_4$ have shown [211] that there seems to be two different pseudogaps: (i) a d-wave-like pseudogap, which is a precursor to superconductivity, near the node of the truly superconducting gap; and (ii) a pseudogap, which became more or less familiar to the community during last years [96,107,187,203–206] and is identified by us as the CDW gap, in the antinodal momentum region. In Reference [212], it was found by ARPES that actually it may be three distinct energy scales, corresponding to pseudogap, fluctuating superconductivity onset and coherence onset temperatures. The authors of Reference [212] also demonstrated that pseudogap competes with d-wave superconductivity in $Bi_2Sr_{2-x}R_xCuO_y$ (R = La and Eu).

Despite existing ambiguities, the most probable description of the competition between CDW gaps (pseudogaps) and superconducting gaps in high-T_c oxides, implies the former emerging at antinodal (nested) sections of the FS, whereas the latter dominating over the nodal sections (See Figure 1, reproduced from Reference [96], where BSCCO was investigated, and results for $(Bi,Pb)_2(Sr,La)_2CuO_{6+\delta}$ [205]). Since CDW gaps are much larger than their superconducting counterparts, the coexistence of both kinds of gaps in the same, antinodal, region might be overlooked in the experiments. This picture means that the theoretical model of partial dielectric gapping (of the CDW origin or caused by the related phenomenon—SDWs) [50–52,61,64,66,68–71,213–216]) is adequate for cuprates.

It is remarkable that similar pseudogaps were also observed in oxypnictides $LaFeAsO_{1-x}F_x$ and $LaFePO_{1-x}F_x$ by ARPES [217] and $SmFeAsO_{0.8}F_{0.2}$ by femtosecond spectroscopy [218], where SDWs might play the same role as CDWs in cuprates. At the same time, in the iron arsenide $Ba_{1-x}K_xFe_2As_2$, photoemission studies detected a peculiar electronic ordering with a $(\pi/a_0, \pi/a_0)$ wave vector [219], a true nature of which is still not known, but which might be related either to the magnetic reconstruction of the electron sub-system (SDWs) or/and to structural transitions (when CDWs in the itinerant electron liquid accompanied by periodic crystal lattice distortions emerge near the structural transition temperature T_d [122,220]). The interplay between structural and magnetic instabilities is important for pnictides [221], since, e.g., structural and SDW anomalies appear jointly at 140 K in $BaFe_2As_2$ [222]. We note that, although CDWs and SDWs are similar phenomena in many respects, their interplay with superconductivity is quite different in what concerns the electron spectrum *per se*, because, instead of a single combined gap at the nested sections. one should deal with two combined gaps corresponding to different spin sublattices [68,213,214].

Figure 1. Schematic illustrations of the gap function evolution for three different doping levels of $Bi_2Sr_2CaCu_2O_{8+\delta}$. (**a**) Underdoped sample with $T_c = 75$ K; (**b**) underdoped sample with $T_c = 92$ K, and (**c**) overdoped sample with $T_c = 86$ K. At 10 K above T_c, there exists a gapless Fermi arc region near the node; a pseudogap has already fully developed near the antinodal region (red curves). With increasing doping, this gapless Fermi arc elongates (thick red curve on the Fermi surface (FS)), as the pseudogap effect weakens. At $T < T_c$ a d-wave like superconducting gap begins to open near the nodal region (green curves); however, the gap profile in the antinodal region deviates from the simple $d_{x^2-y^2}$ form. At $T \ll T_c$, the superconducting gap with the simple $d_{x^2-y^2}$ form eventually extends across the entire FS (blue curves) in (**b**) and (**c**), but not in (**a**). (Taken from Reference [96]).

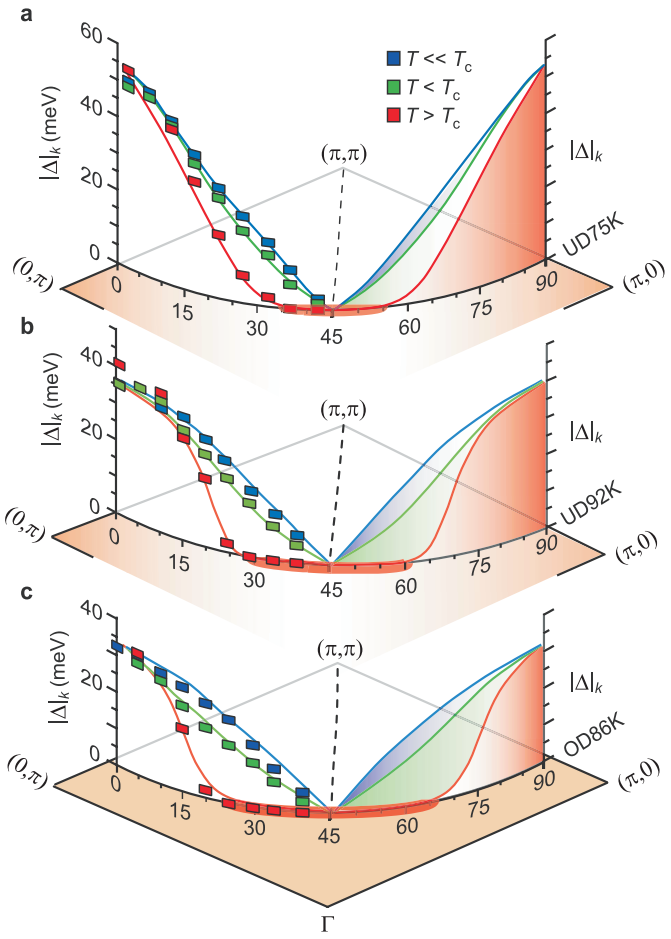

3. Hamiltonian

Our models for the s-wave CDWs + s-wave [60,71,73] or $d_{x^2-y^2}$-wave superconductivity [119–121] are a generalization of earlier theories [50–52,61,64,66,68,69] dealing with the interplay between the isotropic s-wave Cooper pairing and CDWs. Hereafter, we restrict ourselves to the "pure" s- or $d_{x^2-y^2}$-superconductivity bearing in mind that orthorhombic distortions—in particular, for $YBa_2Cu_3O_{7-\delta}$ [223]—allow the appearance of a state with a combined $s + d$ order parameter [23,24]. The coexistence of such a state with CDWs should be rather involved, since, as is shown below, the

phase diagrams are quite different in the mentioned two "pure" cases. Below, we shall refer to them as to the s- and d-cases.

In essence, the CDW superconductor is a combination of two "parent" states: the CDW metal and the BCS superconductor. The corresponding pairing interactions interfere with each other, because of the struggle for the same states on the same FS, ungapped at high enough T (above all relevant critical points). Of course, it might happen, in principle, that the dielectric gap exists up to the highest critical T, when the underlying crystal lattice is stable. Such a situation is suggested, e.g., for narrow-gap $A^{IV}B^{VI}$ semiconductors considered as excitonic phases, with the parent phase existing only as a virtual possibility [224]. This is not the case for cuprates, where the interplay takes place between pairings of approximately equal strength with interesting consequences (see below).

Anyway, the metal FS is partially gapped by CDWs for $T < T_d$ (T_d is the critical CDW-PLD temperature) at the sections (in pairs, j_1 and j_2), which are congruent to each other (nested, d) and where the quasiparticle spectrum $\xi(\mathbf{p})$ is degenerate,

$$\xi_{j_1}(\mathbf{p}) = -\xi_{j_2}(\mathbf{p} + \mathbf{Q}_j) \tag{1}$$

Here, $\mathbf{Q}_j$ are vectors connecting the j-th couple of FS sections. The remaining FS part is non-dielectrized (nd, non-gapped by electron-hole pairing), and its quasiparticle spectrum $\xi_{nd}(\mathbf{p})$ is non-degenerate. The mean-field electron-hole pairing Hamiltonian responsible for CDWs has the form

$$\mathcal{H}_{\mathrm{CDW}} = -\frac{1}{2}\sum_{j=(j_1,j_2)} \Sigma_j(T) \sum_{\mathbf{p};\alpha=\uparrow,\downarrow} a^{\dagger}_{j_1\mathbf{p}\alpha} a_{j_2\mathbf{p}+\mathbf{Q}_j\alpha} + \mathrm{c.c.} \tag{2}$$

Here, the Planck's constant $\hbar = 1$, $a^{\dagger}_{j\mathbf{p}\alpha}(a_{j\mathbf{p}\alpha})$ is the creation (annihilation) operator of a quasiparticle with the momentum $\mathbf{p}$ in the j-th branch of the electron spectrum and with the spin projection $\alpha = \pm\frac{1}{2}$. The quantity $\Sigma_j(T)$ is a T-dependent order parameter of the j-th CDW existing below the relevant critical temperature T_d. We consider it uniform within the corresponding nested FS sections (j_1 and j_2). Summation in Equation (2) is carried out over the dielectrically gapped FS sections only, *i.e.*, over the pairs of sections $j = (j_1, j_2)$ connected by the wave vectors $\mathbf{Q}_j$. In our phenomenological approach, the mechanism of CDW generation [52,122,171–174,220,225,226] is not specified, and any information concerning the strength of dielectric pairing is implicitly contained in the relevant constants $\Sigma_{j0} = \Sigma_j(T = 0)$. In practice, it may be impossible to distinguish between electron-phonon and Coulomb (excitonic) contributions to pairing interactions in Cooper or electron-hole channels. Such a situation has been recently analyzed [227] using the intercalated CDW superconductor Cu_xTiSe_2 [228] and pure $TiSe_2$, which becomes a superconductor under pressure [229], as examples. In what follows, we suggest the simplest case that all quantities $\Sigma_j(T)$ are equal to one another, $\Sigma_j(T) = \Sigma(T)$, and $\Sigma(T = 0) = \Sigma_0$.

As for the parent superconductor, we treat it as a weak-coupling one [230,231] and suggest a strong mixing of states from different FS sections leading to a unique superconducting order parameter $\Delta(T)$ [61,63],

$$\mathcal{H}_{\mathrm{BCS}} = -\sum_{\mathbf{p}} \Delta(T) f(\mathbf{p}) \sum_{j=(j_1,j_2)} a^{\dagger}_{j_1\mathbf{p}\uparrow} a^{\dagger}_{j_2-\mathbf{p}\downarrow} + a^{\dagger}_{nd,\mathbf{p}\uparrow} a^{\dagger}_{nd,-\mathbf{p}\downarrow} + \mathrm{c.c.} \tag{3}$$

The angular factor $f(\mathbf{p})$ depends on the order parameter symmetry. Summation in Equation (3) is executed over the whole FS. The Cooper pairing strength is determined by the parameter $\Delta_0 = \Delta\ (T = 0)$.

The kinetic energy term in the Hamiltonian is conventional, making allowance for all FS sections,

$$\mathcal{H}_0 = \sum_{i=j_1,,j_2,nd} \sum_{\mathbf{p};\alpha=\uparrow,\downarrow} \xi_i(\mathbf{p}) a^{\dagger}_{i\mathbf{p}\alpha} a_{i\mathbf{p}\alpha} \tag{4}$$

The total Hamiltonian of the electron subsystem is a sum of three terms Equations (2)–(4). Further consideration is convenient to be carried out separately for each pairing symmetry.

To make subsequent expressions more compact, let us introduce the following notations: $R_s = [\Delta_0/T_{c0}]_{s-\text{wave}} = \frac{\pi}{\gamma} \approx 1.764$, where $\gamma \approx 1.781$ is the Euler constant, for the ratio between the zero-T gap value and the critical temperature for the BCS s-wave superconductor (it is also appropriate to the ratio Σ_0/T_{d0} between the relevant parameters Σ_0 and T_{d0} of the CDW metal); $R_d = [\Delta_0/T_{c0}]_{d-\text{wave}} = \frac{2}{\sqrt{e}}\frac{\pi}{\gamma} \approx 2.140$, where e is the base of natural logarithms, for the analogous ratio for the BCS d-wave superconductor; and the ratio between those two quantities $\bar{\sigma}_0 = R_s/R_d = \frac{\sqrt{e}}{2} \approx 0.824$. The usage of functions $\text{Mü}_s(T)$ and $\text{Mü}_d(T)$—they describe the T-behavior of the energy gap in s- and d-wave, respectively, superconductors normalized by the gap value at zero temperature—means that they vanish above the corresponding critical temperatures: $\text{Mü}_s(T \geq R_s^{-1} \approx 0.567) = 0$ and $\text{Mü}_d(T \geq R_d^{-1} \approx 0.467) = 0$ (see Figure 2).

Figure 2. Dependences of the normalized order parameters in s- and d-wave Bardeen–Cooper–Schrieffer superconductors (SCs) on the normalized temperature. See explanations in the text.

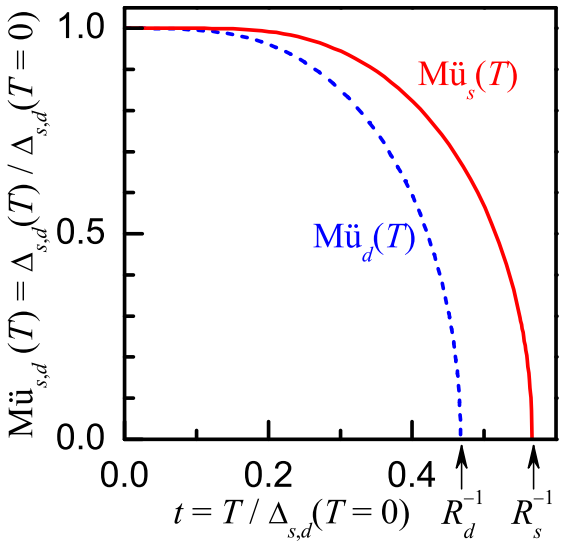

4. s-Wave CDW Superconductor

In this case, $f(\mathbf{p}) = 1$ in Equation (3), and the problem is invariant with respect to rotations in the $\mathbf{p}$-space. Below, we shall analyze the application of the CDW+superconductivity concept to high-T_c oxides, the Brillouin zone of which is two-dimensional. However, owing to the rotational invariance,

the dimensionality is irrelevant in the formulation for the s-case, so that Figure 3 can be considered as a 2D-illustration of both 2D and 3D possible geometries.

Figure 3. Superconducting s-wave (Δ_s, dotted curve) and d-wave (Δ_d, dashed curve), and charge-density wave (CDW, Σ, solid curve) order parameter profiles on the FS in two-dimensional momentum space for the parent phases of the s- or d-wave SC and the CDW metal, respectively, *i.e.*, when the competitive pairing channel is switched off. $\mathbf{Q}_1$ and $\mathbf{Q}_2$ are the CDW vectors, 2α is the opening of each CDW-gapped sectors, β is the mismatch angle between the superconducting lobes and CDW sectors. The checkerboard CDW configuration is described by both wave vectors $\mathbf{Q}_1$ and $\mathbf{Q}_2$, and it includes all four CDW sectors; the unidirectional one is described by one wave vector $\mathbf{Q}_1$, and it includes two hatched CDW sectors.

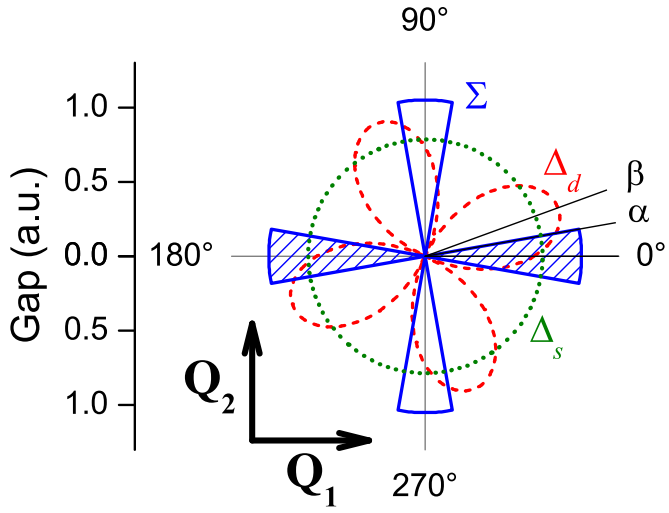

The superconducting gap Δ of the parent s-wave superconductor isotropically spans the whole FS (see curve Δ_s in Figure 3). At the same time, the dielectric gap Σ in the parent CDW metal appears at the nested FS sections separated by the CDW vector $\mathbf{Q}_1$ (the hatched sectors in Figure 3). Owing to the assumption that the quantity $\Sigma(T)$ is identical for all CDW-dielectrized FS sections, there is no matter how many $\mathbf{Q}$-vectors exist in this case and how the corresponding nonoverlapping FS sections are arranged over the FS. The cumulative effect of all nested sections is described by introducing the parameter

$$\mu = \frac{N_d(0)}{N_d(0) + N_{nd}(0)} \tag{5}$$

which corresponds to the degree of the FS dielectric gapping (here, $N_{d,nd}(0)$ are the electron densities of states at the dielectrized and non-dielectrized FS, respectively). The quantities Δ_0, Σ_0, and μ compose the full set of initial parameters for the problem in its s-version, *i.e.*, for the CDW s-wave superconductor.

The many-body correlation effects different from those described by the pairing terms (Equations (2) and (3)) in the Hamiltonian are incorporated into μ, since the very form of the FS calculated in microscopic and semi-microscopic models depends on the many-body electron-electron correlations [93,232,233].

In a standard way [52,71,234], from Dyson–Gor'kov equations, we obtain the Green's functions describing the electron component of our CDW superconductor and insert them into self-consistency equations for the self-energy parts $\Sigma(T)$ and $\Delta(T)$. The formulated problem has the following self-consistent solution [71]. A gap $\Delta(T)$ appears on the non-nested and a gap

$$D(T) = \sqrt{\Delta^2(T) + \Sigma^2(T)} \tag{6}$$

on the nested FS sections. Hence, the superconducting order parameter Δ defines the gap Δ on the nd-section, whereas both order parameters are responsible for the gap D on the d-sections. Since the system of coupled equations can be formulated in terms of the gaps (Δ, D) rather than the order parameters (Δ, Σ), it can be decoupled into separate equations: for the gap Δ,

$$I_M(\Delta, T, \Delta(0)) = 0 \tag{7}$$

and the combined gap D,

$$I_M(D, T, \Sigma_0) = 0 \tag{8}$$

Here, the Boltzmann constant $k_B = 1$,

$$\Delta(0) = \left(\Delta_0 \Sigma_0^{-\mu}\right)^{\frac{1}{1-\mu}} \tag{9}$$

the quantity

$$I_M(\Delta, T, \Delta_0) = \int_0^\infty \left(\frac{1}{\sqrt{\xi^2 + \Delta^2}} \tanh \frac{\sqrt{\xi^2 + \Delta^2}}{2T} - \frac{1}{\sqrt{\xi^2 + \Delta_0^2}} \right) d\xi \tag{10}$$

is the so-called Mühlschlegel integral [235], and the solution $\Delta(T) = \Delta_0 \mathrm{M\ddot{u}}_s(T/\Delta_0)$ of the equation $I_M(\Delta, T, \Delta_0) = 0$ is the well-known T-function for the gap in the conventional BCS s-wave theory (see Figure 2).

Equations (7) and (8) evidence that both self-consistent *gaps* behave as if they were independent, possessing the T-dependence of the s-wave BCS theory. Nevertheless, the mutual interdependence between the order parameters Δ and Σ is preserved. First, Equation (6) demonstrates that superconductivity inhibits CDWs in the range of their coexistence by reducing the value of the dielectric order parameter Σ in comparison with its pristine value $\Sigma = \Sigma_0 \mathrm{M\ddot{u}}_s(T/T_d)$ in the parent CDW metal. Second, the CDW actively participate in the formation of the $\Delta(T)$-dependence by forming its maximum value at $T = 0$ (see Equation (9)). Both phenomena are illustrated in Figure 4.

Figure 4. Normalized-temperature, t, dependences of the normalized s-wave SC and CDW order parameters as functions of (**a**) the dielectric gapping degree μ; and (**b**) the ratio $\sigma_0 = \Sigma_0/\Delta_0$ between the parent pairing parameters.

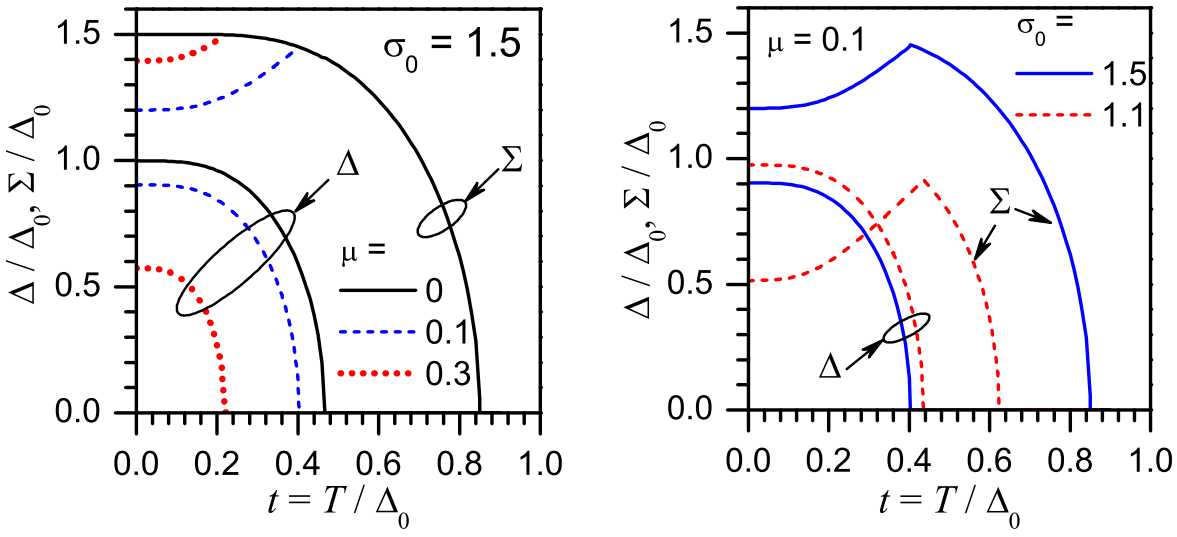

(**a**) (**b**)

The phase diagram for the s-wave CDW superconductor in the $\sigma_0 - \mu$ plane is rather simple (Figure 5). It is clear that the maximal—between T_{c0} and T_{d0}—parent temperature remains the actual one. However, in the framework of our model, due to the strong mixing of the electron states between different FS sections [61], the superconducting gap Δ occupies the whole FS. Therefore, if $T_{c0} > T_{d0}$, which means that $\Delta_0 > \Sigma_0$, *i.e.*, $\sigma_0 < 1$, the superconductivity is "stronger" than the electron-hole pairing at any $T < T_{c0}$, *i.e.*, $\Delta(T)$ for a parent superconductor is larger than $\Sigma(T)$ for a parent CDW metal, and it gives no chance for the latter to develop. Hence, the portion of the phase diagram to the left from the line $\sigma_0 = 1$ is an area, where CDWs are totally suppressed, the same being true for the whole x-axis ($\mu = 0$). On the other hand, it is also clear that a configuration of partial dielectric gapping implies the existence of an nd-section (an "open back door") on the FS, through which superconductivity could always "find its way". Therefore, the partially gapped CDW s-superconductor preserves superconductivity at almost every point of the presented phase diagram. The only exception is case of full FS dielectrization, $\mu = 1$, together with the condition $\sigma_0 > 1$, when the emerging CDWs results in the metal-insulator transition.

Figure 5. Phase diagram of the CDW s-superconductor on the $\mu - \sigma_0$ plane. The grey region corresponds to the pure SC phase, where CDWs are absent at any T. The bold line denotes the pure CDW phase. The rest of the plane corresponds to the combined SC + CDW phase. Critical CDW isotherms are shown by solid and SC ones by dashed curves. See explanations in the text.

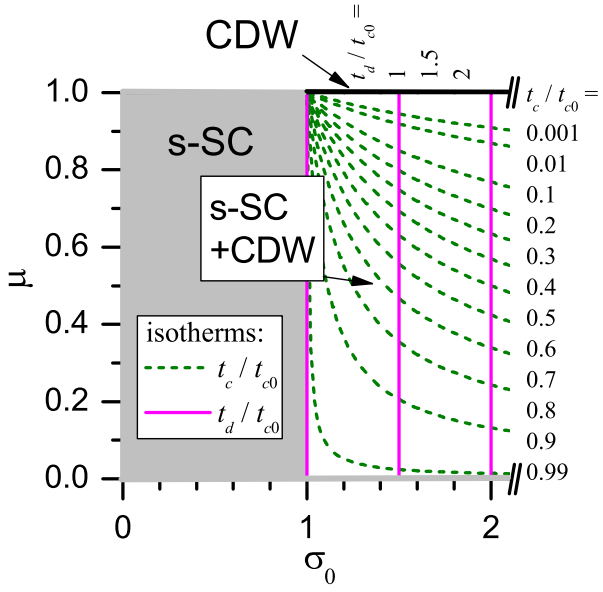

Since

$$\frac{T_d}{T_{c0}} = \frac{T_d}{\Sigma_0}\frac{\Sigma_0}{\Delta_0}\frac{\Delta_0}{T_{c0}} = \frac{\gamma}{\pi}\frac{\Sigma_0}{\Delta_0}\frac{\pi}{\gamma} = \sigma_0 \tag{11}$$

it is clear that T_d-isotherms on the phase diagram are parallel $\sigma_0 = const$-lines. On the other hand, using Equation (9), one obtains

$$\frac{T_c}{T_{c0}} = \frac{T_c}{\Delta(0)}\frac{\Delta(0)}{\Delta_0}\frac{\Delta_0}{T_{c0}} = \frac{\gamma}{\pi}\frac{\left(\Delta_0\Sigma_0^{-\mu}\right)^{\frac{1}{1-\mu}}}{\Delta_0}\frac{\pi}{\gamma} = \sigma_0^{-\frac{\mu}{1-\mu}} \tag{12}$$

The corresponding normalized T_c and T_d isotherms are depicted in Figure 5.

Taking into account our further presentation, it is worth noting two circumstances. First, according to Equation (7), the ratio $\Delta(0)/T_c$ preserves its s-BCS value $R_s = \frac{\pi}{\gamma}$. Second, in the range of CDW + s-BCS coexistence ($\sigma_0 > 0$) and according to Equation (9), we have $0 < \Delta(0) < \Delta_0 < \Sigma_0$. Together with Equation (6), it leads to $\Sigma(T = 0) > 0$, so that the dielectric order parameter Σ is always nonzero within the whole temperature interval $0 \leq T < T_d = T_{d0}$.

5. d-Wave CDW Superconductor. Formulation

In this case, taking into account that we intend to analyze high-T_c oxides, the consideration may be carried out in the 2D p-space. Since the problem becomes anisotropic from the very beginning, its further specifications are needed.

Experimentally, two CDW configurations are observed in high-T_c oxides. In the unidirectional one, there exists a single CDW described by a single wave vector $\mathbf{Q}_1$. In the checkerboard configuration, there

are two CDWs described by two mutually orthogonal vectors $\mathbf{Q}_1$ and $\mathbf{Q}_2$ with equal magnitudes. Both geometries are depicted in Figure 3. We adopt that the CDW vector $\mathbf{Q}_1$, which connects two dielectrically gapped FS sections in the unidirectional geometry (this case is marked by hatched lobes) is parallel to the p_x-axis. Each section has the angular width 2α, independent of the temperature T. Two more gapped sections are added about the p_y-axis in the case of checkerboard geometry, characterized by two mutually perpendicular CDW vectors $\mathbf{Q}_1$ and $\mathbf{Q}_2$ (four lobes with a solid boundary in Figure 3). We adopt that, except the orientation, the nested FS section are identical, being measured by the same angle 2α and dielectrically gapped to the same uniform amplitude $\Sigma(T)$. The sections are located symmetrically with respect to the corresponding axes, so that the bisectrices of dielectrically gapped sectors—in such a way, we fix the positions of the nested FS sections—coincide with the axes. Here, we may also introduce the parameter μ, which describes the degree of FS gapping. But, as it will be seen, another choice turns out to be more convenient.

Note that CDWs in the Hamiltonian term Equation (2) are assumed thereafter to have s-wave symmetry, although their testing ground is restricted to the hot spots (4 or 2 sectors with 2α openings as is clear from Figure 3). On the other hand, certain experimental data were suggested to testify the validity of the d-wave scenario for CDWs [236–238], emphasizing, in their opinion, an underlying kinship between superconductivity and charge ordering. Since measurements indicating d- rather than s-wave symmetry of pseudogaps (CDW gaps) in cuprates are rare and inconclusive from the viewpoint of the symmetry identification (see, e.g., References [96,134,239] containing contradicting experimental evidence), we consider $\Sigma(T)$ angle-independent (s-wave like) inside the corresponding sectors in the $\mathbf{p}$-space. Nevertheless, a d-wave dielectric order parameter can happen in other materials, so that theoretical efforts in this direction [240–248] are justified.

As for the distribution of the superconducting gap Δ over the FS of the parent d-superconductor in the 2D geometry, the corresponding angular factor in Equation (3) has the form $f(\mathbf{p}) = \cos 2\theta$, where the angle θ is reckoned from a certain direction in the 2D momentum space denoted by the angle β. In the $d_{x^2-y^2}$-state, the Δ-lobes are directed along the p_x- and p_y-axes [249,250], so that the mismatch angle β between the "superconducting" and "dielectric" lobes in the parent metal is zero ($\beta = 0$). Moreover, according to the experiment, the sectors with non-zero pseudogap (in our interpretation, the CDW gap, Σ) are competing with superconductivity exactly in those, the most vulnerable to the obstacle, antinodal regions [96,112,185,205,239]. (It is those FS sections in high-T_c cuprates that are sometimes coined "hot spots" [93,125,126,251,252]). Nevertheless, we would like to extend the range of system parameters and consider also the case with a loss of symmetry $\beta \neq 0$, a more general model than that describing actual hole-doped cuprates. Thus, we assume that the CDW directions remain fixed with respect to the background crystal lattice. At the same time, the superconducting lobes can be rotated by the angle β around the 2D Brillouin zone axis. Note that if $\beta = \frac{\pi}{4}$, the superconducting state becomes the hypothetical d_{xy} one with an underlying symmetry restored [5,23,24,133,250,253]. In all the intermediate states with $\beta \neq 0$ or $\frac{\pi}{4}$, the conventional angular symmetry is broken, but such so far hypothetical states might exist in real distorted crystals, as well as under an applied non-hydrostatic external pressure. This picture is appropriate to the checkerboard situation, while for the unidirectional configuration we actually deal with stripe patterns [254] with a certain loss of symmetry, although

without any antiferromagnetic domains (stripes) appropriate to the original stripe scenario [141,149]. It turned out to be instructive to compare both cases.

It is evident that the problem is invariant with respect to the system rotation in the momentum space by the angle $\Omega = \pi$ in the unidirectional case with the number of CDW sectors $N = 2$, and $\Omega = \frac{\pi}{2}$ in the checkerboard one with the number $N = 4$. It is easy to see that the parameters μ, α, N, and Ω are linked by the relations

$$\mu\Omega = 2\alpha \tag{13}$$

$$N\Omega = 2\pi \tag{14}$$

Those formulas demonstrate that the parameter α can vary from 0 ($\mu = 0$, the absence of FS dielectric gapping) to $\frac{\pi}{2}$ in the unidirectional CDW configuration (the case of full FS gapping, $\mu = 1$, and $N = 2$) and to $\frac{\pi}{4}$ in the checkerboard one ($\mu = 1$, $N = 4$). As we shall see below, the gapping degree parameter α is more demonstrative here than μ, contrary to the case of isotropic CDW superconductors [71].

The total Hamiltonian of the electron subsystem is a sum of three terms Equations (2)–(4). The quantities Σ_0, Δ_0, μ (or α), Ω (or N), and the mismatch angle β between the bisectrices of CDW sectors and superconducting lobes constitute the full set of the problem input parameters. They are phenomenological constants that can be, in principle, reconstructed from the experimental data. For instance, such a possibility exists for the ratio μ between the dielectrized portion of the FS and the total length of the FS in the 2D Brillouin zone.

The technique of derivation of relevant Green's functions and the self-consistency equations for the self-energy parts $\Sigma(T)$ and $\Delta(T)$ is the same as was used in the s-case. However, now we can obtain separate equations neither for the order parameters (Δ, Σ) nor for their certain combinations like Equation (6). It is convenient to introduce the dimensionless temperature $t = T/\Delta_0$ and order parameters $\sigma(t) = \Sigma(T)/\Delta_0$ ($\sigma_0 = \Sigma_0/\Delta_0$) and $\delta(t) = \Delta(T)/\Delta_0$ ($\delta_0 \equiv 1$). Then, the relevant equations look like

$$\int_{-\alpha}^{\alpha} I_M(\sqrt{\sigma^2 + \delta^2 \cos^2 2(\beta + \theta)}, t, \sigma_0) d\theta = 0 \tag{15}$$

$$\frac{8}{N} \int_0^{\pi/4} I_M(\delta \cos 2\theta, t, \cos 2\theta) \cos^2 2\theta d\theta + \int_{\beta-\alpha}^{\beta+\alpha} \left[I_M(\sqrt{\sigma^2 + \delta^2 \cos^2 2\theta}, t, \cos 2\theta) - I_M(\delta \cos 2\theta, t, \cos 2\theta) \right] \cos^2 2\theta d\theta = 0 \tag{16}$$

If superconductivity is absent ($\delta = 0$), Equation (15) is reduced to the gap equation for the parent CDW metal [77]

$$I_M(\sigma, t, \sigma_0) = 0 \tag{17}$$

and its solution is $\sigma(t) = \sigma_0 \mathrm{M\ddot{u}}_s(t)$. At the same time, when the dielectrization is absent ($\sigma = 0$ or $\alpha = 0$), Equation (16) becomes the equation for a d-wave BCS weak-coupling superconductor

$$\int_0^{\pi/4} I_M(\delta \cos 2\theta, t, \cos 2\theta) \cos^2 2\theta d\theta = 0 \tag{18}$$

and its solution is $\delta(t) = \text{Mü}_d(t)$. (See the corresponding curves in Figure 2, as well as References [230,231,234,255].)

Below we are going to construct the overall phase diagram of the CDW d-superconductor on the $\sigma_0 - \alpha$ plane. The mismatch angle β describes a possible symmetry breaking, if $\beta \neq 0$ or $\frac{\pi}{4}$ (checkerboard case) , or $\beta \neq 0$ or $\frac{\pi}{2}$ (unidirectional case). For cuprates, experimental data demonstrate that $\beta = 0$ [96,185,205,239].

6. d-Wave Superconductor. Phase Diagram Boundaries

Let us construct specific phase diagrams for CDW d-superconductors on the $\sigma_0 - \alpha$ plane. It is clear that this situation should differ from the s-wave one, owing to two circumstances. First, the dependence $\text{Mü}_d(t)$ is steeper than the $\text{Mü}_s(t)$ one (see Figure 2). Within the interval $\bar{\sigma}_0 < t < 1$, the parent dielectric order parameter Σ_0 is larger than Δ_0, although $T_{d0} < T_{c0}$. Therefore, d-wave superconductivity, being more vigorous, may dominate at low temperatures, which is really the case. At the same time, the presence of superconducting gap nodes on the FS makes d-superconductivity less "resistive" against the penetration of CDW gaps onto FS in the areas of the phase diagrams, where $T_{c0} > T_{d0}$. It is precisely the region to the left from the line $\sigma_0 = \bar{\sigma}_0$. It is clear that this effect must be more pronounced for $\beta \neq 0$, especially at $\beta \to \frac{\pi}{4}$.

As has been indicated above, the mismatch angle β describes a possible symmetry breaking in the cases $\beta \neq 0$ or $\frac{\pi}{4}$ (checkerboard case), or $\beta \neq 0$ or $\frac{\pi}{2}$ (unidirectional case). For cuprates, experimental data demonstrate that $\beta = 0$ [96,185,205,239]. A pattern with a broken symmetry might be due to internal residual strains in the sample, a non-homogeneous distribution of the dopant atoms, an influence of out-of-plane structural elements (such as chains in $YBa_2Cu_3O_{7-\delta}$ [124,142]) or the deliberate switching on of external factors, e.g., uniaxial pressure.

It is worth mentioning that the choice of the dimensionless parameter $\sigma_0 = \Sigma_0/\Delta_0$—*i.e.*, the normalization by $\Delta_0 \neq 0$—implies the obligatory existence of Cooper pairing in the system concerned, irrespective of whether the mechanism of dielectric pairing is engaged or not. Thus, all possible (σ_0, α)-combinations at a fixed β fill the whole semi-infinite ($\sigma_0 \geq 0$) strip on the $\sigma_0 - \alpha$ plane between the ordinates $\alpha = 0$ and $\frac{\pi}{4}$, in the case of the checkerboard CDW configuration, and between $\alpha = 0$ and $\frac{\pi}{2}$, in the case of the unidirectional one. Since the former case is observed much more frequently, we shall analyze it first.

Two loci in the $\alpha - \sigma_0$ phase diagram are trivial, both corresponding to the total absence of CDWs. These are (see Figure 6) the case $\alpha = 0$ (the positive abscissa semi-axis) and the case $\sigma_0 = 0$ (the whole sector $0 \leq \alpha \leq \frac{\pi}{4}$ in the checkerboard configuration), corresponding to the ordinate axis (α-axis). Both lines represent the parent d-BCS superconductor. It is also clear that, as it was in the s-case, except for the limiting case of complete FS dielectrization, superconductivity could always penetrate onto the FS owing to the availability of nd-section. Again, the partially gapped CDW d-superconductor preserves superconductivity at almost every point of its phase diagram, the value of T_c being another matter. In any case, two main questions are to be answered: (i) To what extent can CDWs suppress superconductivity? and (ii) Can superconductivity completely destroy CDW-PLD?

The third border-line of the phase diagram (part of the straight segment $\alpha = \frac{\pi}{4}$ in the checkerboard case and $\alpha = \frac{\pi}{2}$ in the unidirectional one), which corresponds to the case of complete FS dielectrization, will be considered in Section 9 in more detail.

Figure 6. Phase diagram of the CDW $d_{x^2-y^2}$-superconductor ($\beta = 0°$) in the checkerboard configuration on the $\alpha - \sigma_0$ plane. The grey region corresponds to the pure SC phase, where CDWs are absent at any T, the hatched one to the combined SC+CDW phase, and the CDW-reentrance (cross-hatched) one to the phase, where the superconductivity and CDWs coexist in a certain T-interval $0\ \mathrm{K} < T_\mathrm{r} < T < \min(T_\mathrm{d}, T_\mathrm{c})$. Here, T_r and T_d are the lower and upper CDW critical temperatures, respectively, and T_c is the SC critical temperature. The bold black line along the upper phase diagram boundary denotes the range of pure CDW phase existence. The scaled-up fragment of the phase diagram is shown in the inset.

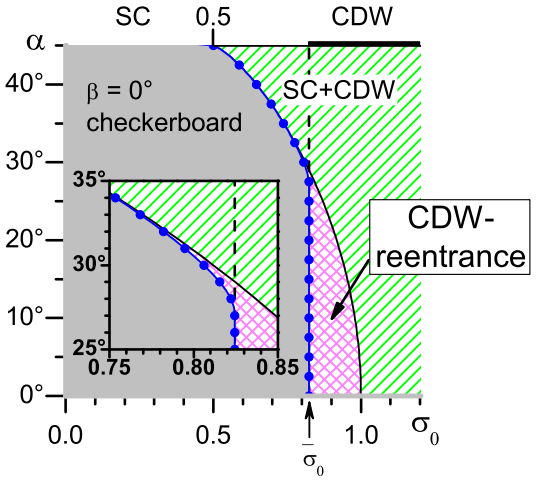

7. Checkerboard CDW Configuration. $d_{x^2-y^2}$-Symmetry of the Superconducting linebreak Order Parameter

Due to different T-behavior of the parent order parameters (see Figure 2) the CDW d-wave superconductor demonstrates a new type of T-dependence, namely, the T-reentrance. In particular, when T decreases, $\Delta(T)$ can grow so sharply in comparison with the CDW competitor $\Sigma(T)$ that the latter becomes totally suppressed at low T, manifesting itself only within a certain "reentrance" interval located in between two nonzero temperatures, T_r and T_d, which depend on the problem parameters. For illustration, consider a scan of the $\sigma_0 - \alpha$ phase plane along a definite path, e.g., $\alpha = 13.5°$, moving from large σ_0-values (see Figure 7). First, when σ_0 is large, $\Delta(T)$- and $\Sigma(T)$-profiles are similar to those obtained in the s-wave case (see Figure 4). Then, for a certain σ_0^{**} ($\sigma_0^{**} \approx 0.9628$ at $\alpha = 13.5°$), $\Sigma(T)$-dependence acquires a dome shape. The further reduction of σ_0 results in a shrinkage of this dome followed by its collapse (the temperatures T_r and T_d converge to $T^* = T_{c0}$) at $\sigma_0^* = \bar{\sigma}_0$. At $\sigma_0 < \bar{\sigma}_0$, d-superconductivity totally inhibits CDWs and we obtain a pristine d-BCS phase.

Figure 7. Normalized temperature dependences of the CDW, Σ, (**a**) and superconducting, Δ; (**b**) order parameters for various σ_0 in the checkerboard configuration. t^* is the normalized reentrance-collapse temperature. See explanations in the text.

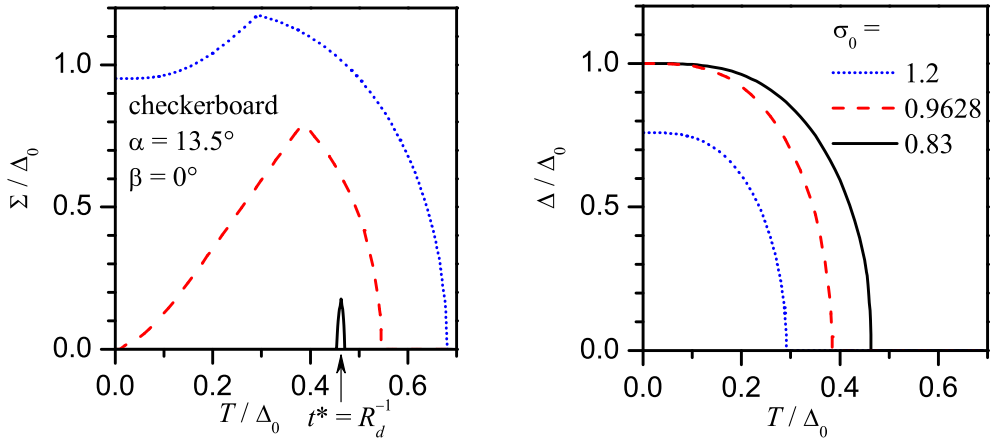

If we scan the whole phase plane in such a manner, we obtain the phase diagram of the partially gapped CDW $d_{x^2-y^2}$-superconductor depicted in Figure 6. The difference between this phase diagram and that for the partially gapped CDW s-superconductor is obvious. As was mentioned above, the dissimilarity stems from different temperature and angular dependences of the parent superconducting gaps Δ in those two cases.

It should be noted that the $\Sigma(T)$-dome collapses to $T^* = T_{c0}$ only within the α-range from 0 to approximately $27.1°$. At larger α, the collapse point shifts towards smaller σ_0, which is illustrated in Figure 8 Accordingly, the collapse temperature T^* also decreases.

Figure 8. The same as in Figure 7, but for $\alpha = 28.5°$.

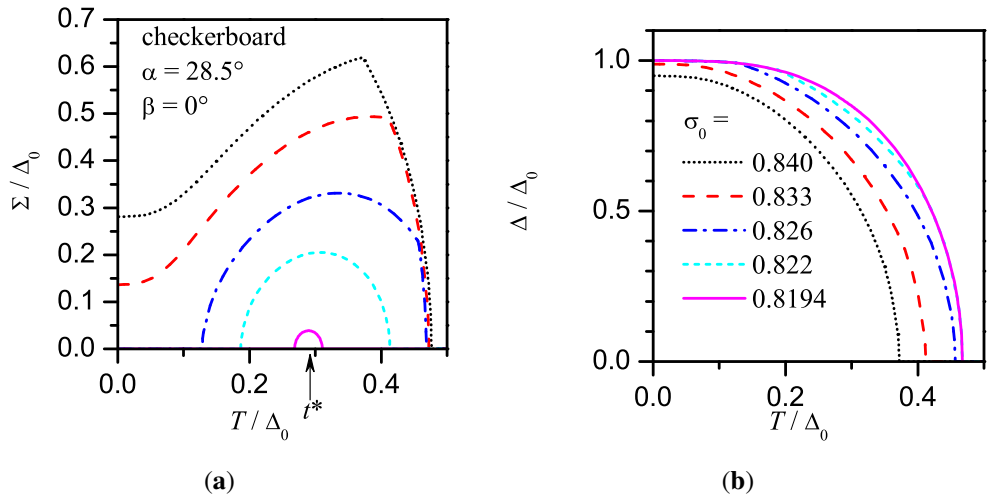

Our calculations testify that the CDW-reentrance region crosses the whole phase plane, although its width becomes very narrow at large α ($\alpha \gtrsim 30°$).

Figure 9 demonstrates the pattern of T_c- and T_d-isotherms in the most interesting region of the phase diagram. One sees that CDWs suppress superconductivity by lowering T_c-values.

Figure 9. Normalized $T_{\rm d}$- and $T_{\rm c}$-isotherms on the phase plane in the checkerboard CDW configuration for $\beta = 0°$.

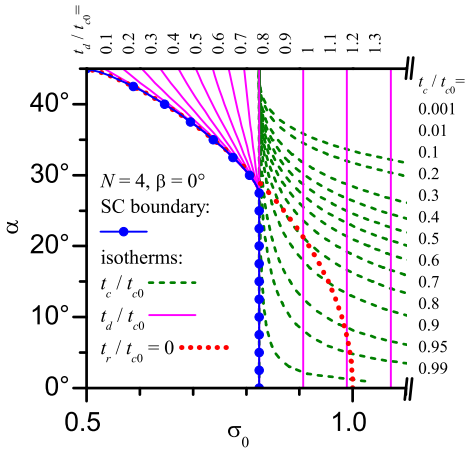

The phase diagram obtained here and displayed in Figure 6 enables us to obtain a certain insight into the mechanism of the $\Sigma(T)$-reentrance governed by the FS dielectric gapping parameter μ. For this purpose, we advanced the representing point along the line $\sigma_0 = 0.9$ on the phase diagram (see Figure 10). A detailed analysis on the basis of Figure 6 shows that while moving along this line from large $\mu \approx 1$ ($\alpha \approx \frac{\pi}{4}$) we meet the same sequence of phases (SC+CDW $\rightarrow$ CDW-reentrance) as if moving along the path $\alpha = \text{const}$ from larger to smaller σ_0 values.

Figure 10. The same as in Figure 7 but for $\sigma_0 = 0.9$ and $\mu = 0.1$ (1), 0.3 (2), 0.5 (3), 0.6 (4).

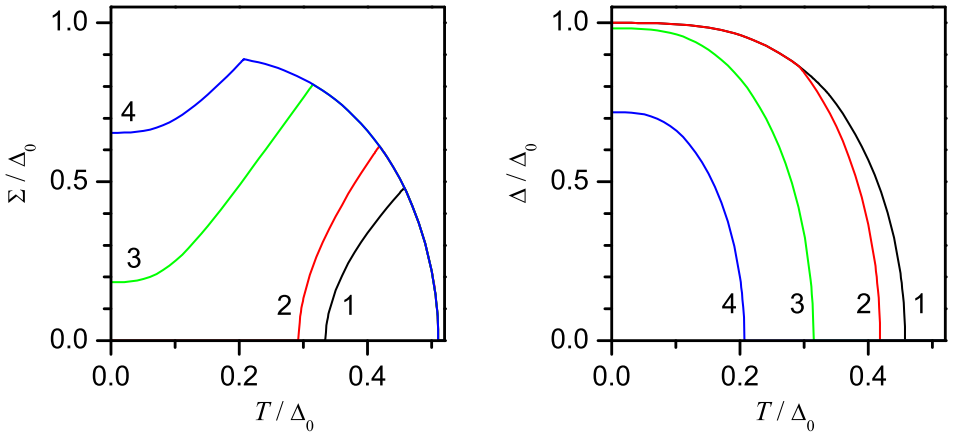

In other words, the calculations demonstrate that an appearance and subsequent gradual destruction of the $\Sigma(T)$ dome, existing for σ_0 both above and below the value $\bar{\sigma}_0$, may be carried out by decreasing α. In the CDW-reentrance region to the right from $\sigma_0 = \bar{\sigma}_0$, the pure superconducting phase is reached only at $\alpha = 0$.

The analysis of the phase diagram would have been incomplete, if one had not paid attention to the behavior of the resulting energy gaps being observable both in tunnel and photoemission spectroscopies. Indeed, even the reentrance of $\Sigma(T)$ does not mean that the overall gap on the FS disappears with lowering T. Examples of the T-evolution of the gaps on non-dielectrized and dielectrized FS sections are shown in Figures 11(a) and 12(a) for two distinctive regimes (with and without the reentrance) realized for different σ_0. The diagrams, which we call hereafter the "gap rose", indicate how complicate may be the pattern probed by cuts from ARPES measurements. On the other hand, the full set of photoemission studies of a certain CDW superconducting sample should reveal bands of gaps of a complicated shape if an angular sweep is made, as is displayed in the corresponding panels (b). As is readily seen, the bands are strongly T-dependent.

Figure 11. (**a**) "Gap rose" in the momentum space at normalized temperatures $t = 0.15$ (solid), 0.3 (short-dashed), 0.4 (long-dashed), 0.5 (dash-dotted curve); (**b**) T-dependences of CDW (solid curve) and SC (dashed curve) order parameters and gap bands (obtained at the angular scanning in the momentum space) on dielectrized (right hatch) and non-dielectrized (left hatch) Fermi surface (FS) sections. In both panels $\mu = 0.3$, $\beta = 0°$, anf $\sigma_0 = 0.95$.

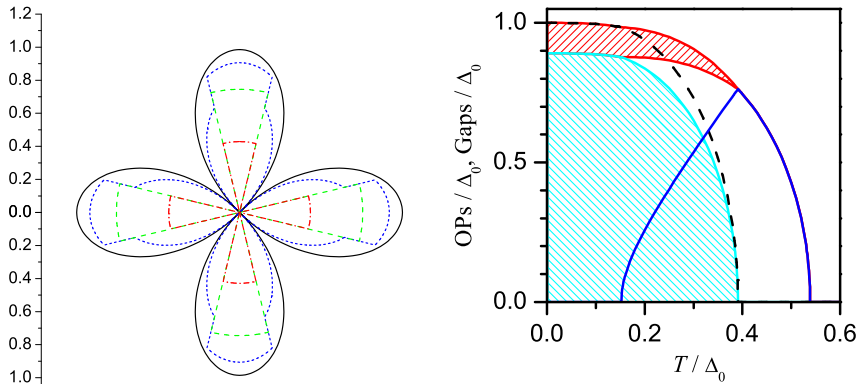

(**a**) (**b**)

Figure 12. The same as in Figure 11, but for $\sigma_0 = 1.2$. Gap roses in panel (**a**) are drawn for $t = 0$ (solid), 0.25 (short-dashed), 0.6 (long-dashed), and 0.65 (dash-dotted curve).

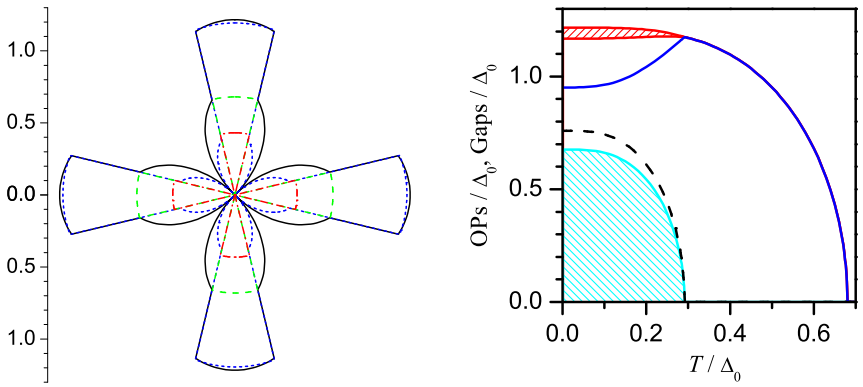

(**a**) (**b**)

It comes about from Figure 10 (a) that one can control the reentrance by changing the parameter μ (*i.e.*, the dielectric sector opening 2α). In its turn μ can be modified by doping [96,205] or applied external pressure, which was demonstrated for other classes of CDW superconductors [256–259]. In the case of cuprates a strong influence on T_c of the uniaxial pressure was disclosed for the oxide $La_{1.64}Eu_{0.2}Sr_{0.16}CuO_4$ near the threshold of the CDW- (stripe-) instability [260].

8. Checkerboard CDW Configuration. Deviations from $d_{x^2-y^2}$-Symmetry

Although this case ($\beta \neq 0$) may seem to some extent academic, we would like to briefly present the corresponding results.

Figure 13(a) demonstrates the evolution of the phase diagram with varying β. One can see that the reentrance region gets narrowed and does not span anymore the whole phase plane. If we present the reentrance regions as triangles with strongly distorted lateral sides, the β-induced changes can be traced as the variation of the height (the ordinate of the phase diagram point, where the boundaries of the reentrance region converge) and the base (the difference $\sigma_0^{**} - \sigma_0^{*}$ between the reentrance-start and reentrance-collapse σ_0-values at $\alpha \to 0$) of those triangles (Figure 13(b)).

Figure 13. (**a**) Phase diagrams for the checkerboard CDW configuration and various mismatch angles β. The dashed curve is the locus of the reentrance-collapse points. See explanations in the text; (**b**) β-dependences of the base (solid curve) and the "height" α (dashed curve) of the reentrance-collapse region.

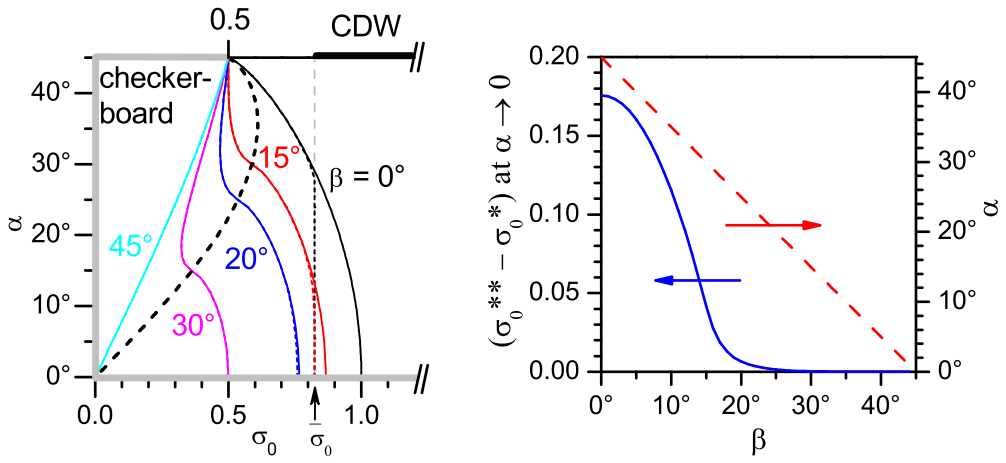

Now, paths along $\alpha = const$ appear, which do not cross the reentrance region, passing over the boundary-convergence point. The corresponding example (Figure 14) shows that CDWs do not disappear within the whole temperature interval below T_d, and the Σ-dome uniformly collapses to the coordinate origin as σ_0 decreases.

Figure 14. The same as in Figure 7 but for $\alpha = 30°$ and $\beta = 20°$.

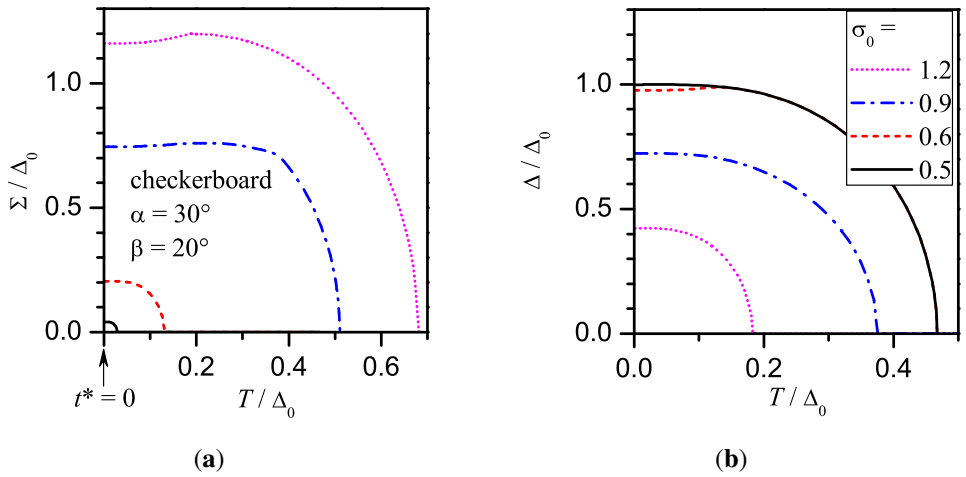

The analysis of Figure 13 shows that, at relatively large β, another kind of Σ-reentrance can take place (reentrance of kind II). Specifically, at a fixed σ_0—e.g., $\sigma_0 = 0.4$—an initial modest increase of the opening angle α from zero does not move the phase point out of the pure SC region. A further increase of α forces the system to become a CDW superconductor, which persists within a certain α-interval. A subsequent growth of α restores the BCS superconducting state.

The most interesting here is the angle $\beta = \frac{\pi}{4}$, which corresponds to the hypothetical case of d_{xy}-pairing. Figure 13 shows that the reentrance region is absent in this case. The corresponding T_c and T_d isotherms are shown in Figure 15. Two examples of gap roses are depicted in Figure 16.

Figure 15. The same as in Figure 9, but for $\beta = 45°$.

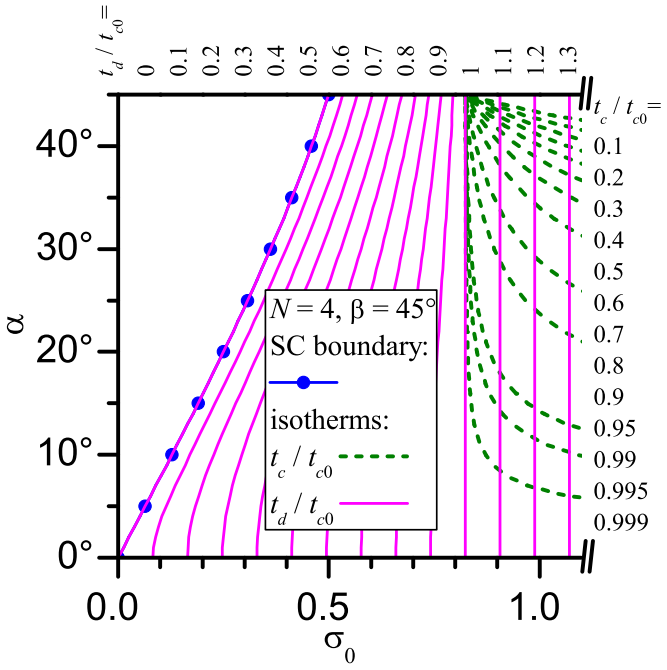

Figure 16. Gap roses at various temperatures and $\alpha = 20°$ for CDW d_{xy}-wave superconductor ($\beta = \frac{\pi}{4}$) with $\sigma_0 = 0.5$ (**a**) and 1.2 (**b**).

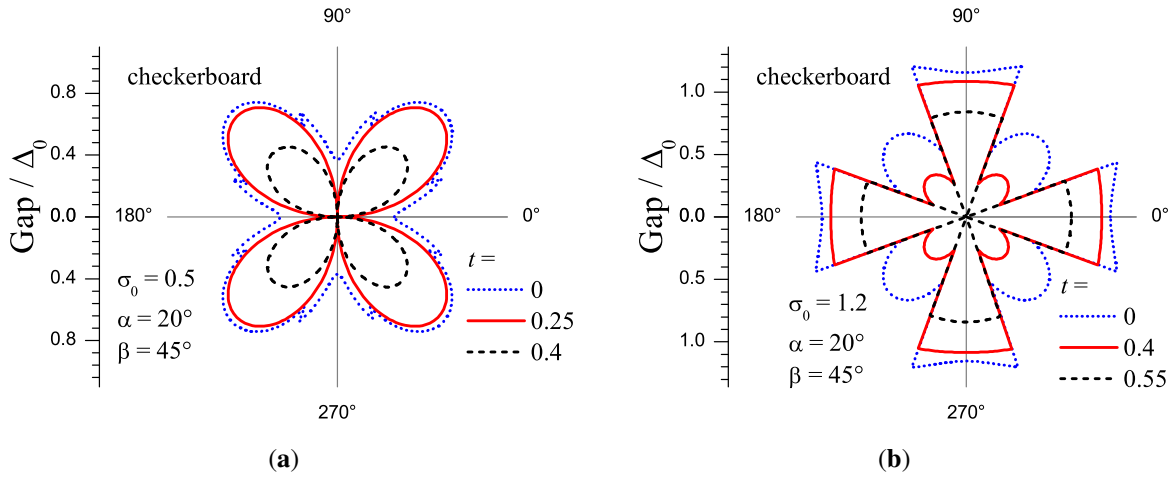

9. Complete FS Dielectrization

In this case, the picture turns out degenerate with respect to the parameter β, the latter becoming irrelevant. Hence, σ_0 remains the only problem parameter.

For completely gapped CDW s-superconductors, only one order parameter survives the competition (see Figure 5, $\mu = 1$). For its $d_{x^2-y^2}$-counterpart (Figure 6, $\alpha = \frac{\pi}{4}$), as a consequence of their different symmetries, Δ and Σ may coexist within the interval

$$\frac{1}{2} < \sigma_0 < \bar{\sigma}_0 \tag{19}$$

It is remarkable that the zero-temperature values $\Delta(0)$ and $\Sigma(0)$ can be obtained analytically [121]:

$$\begin{aligned} \delta(0) &= 2\sigma_0\sqrt{1 - 2\ln(2\sigma_0)} \\ \sigma(0) &= 2\sigma_0 \ln(2\sigma_0) \end{aligned} \tag{20}$$

The dependences $\Sigma(T)$ and $\Delta(T)$ for d-wave superconductors completely gapped by CDWs are depicted in Figure 17. Notice an unexpected reverse analogy to the previous results for the coexistence of isotropic pairings. Namely, T-dependences of CDW (superconducting) order parameters are qualitatively similar to those for their superconducting (CDW) counterparts, respectively, inherent to partially gapped CDW s-superconductors [71]. The T-evolution of gap roses for certain σ_0's is depicted in Figure 18. Figures 17 and 18 illustrate how the parameter σ_0 controls the process of transformation between a BCS superconductor with d-wave Cooper pairing and a CDW metal with s-wave electron-hole pairing. If σ_0 goes close to the limit $\frac{1}{2}$ (Figure 18(a)), the gap configuration has a well pronounced lobe structure, whereas at $\sigma_0 \to \bar{\sigma}_0$ (Figure 18(c)) it tends to the isotropic pattern. Besides, Figure 18(b) demonstrates that the combined gap (at $\mu = 1$, the area available to both order parameters extends over the whole FS) can also reveal a nonmonotonic dependence on T (see gap roses at $t = 0$ and 0.2 in the vicinity of their maxima).

Figure 17. The same as in Figure 7, but for the complete FS dielectric gapping.

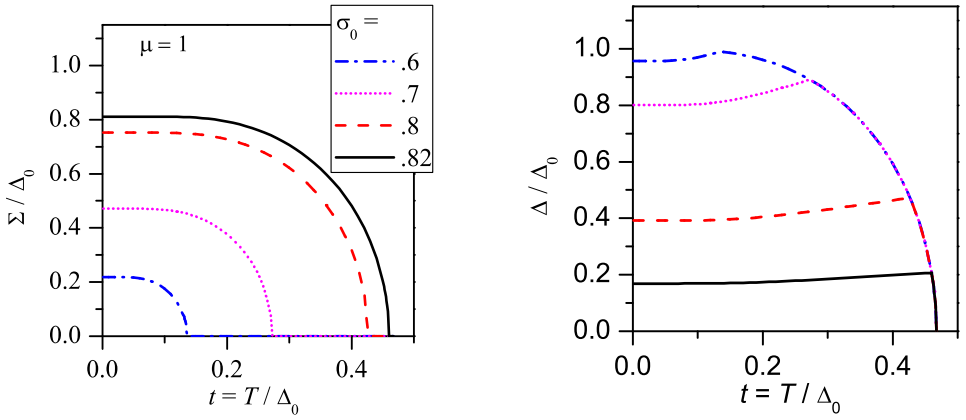

(**a**) (**b**)

Figure 18. Temperature evolution of gap roses at various σ_0 in the case of complete FS dielectric gapping.

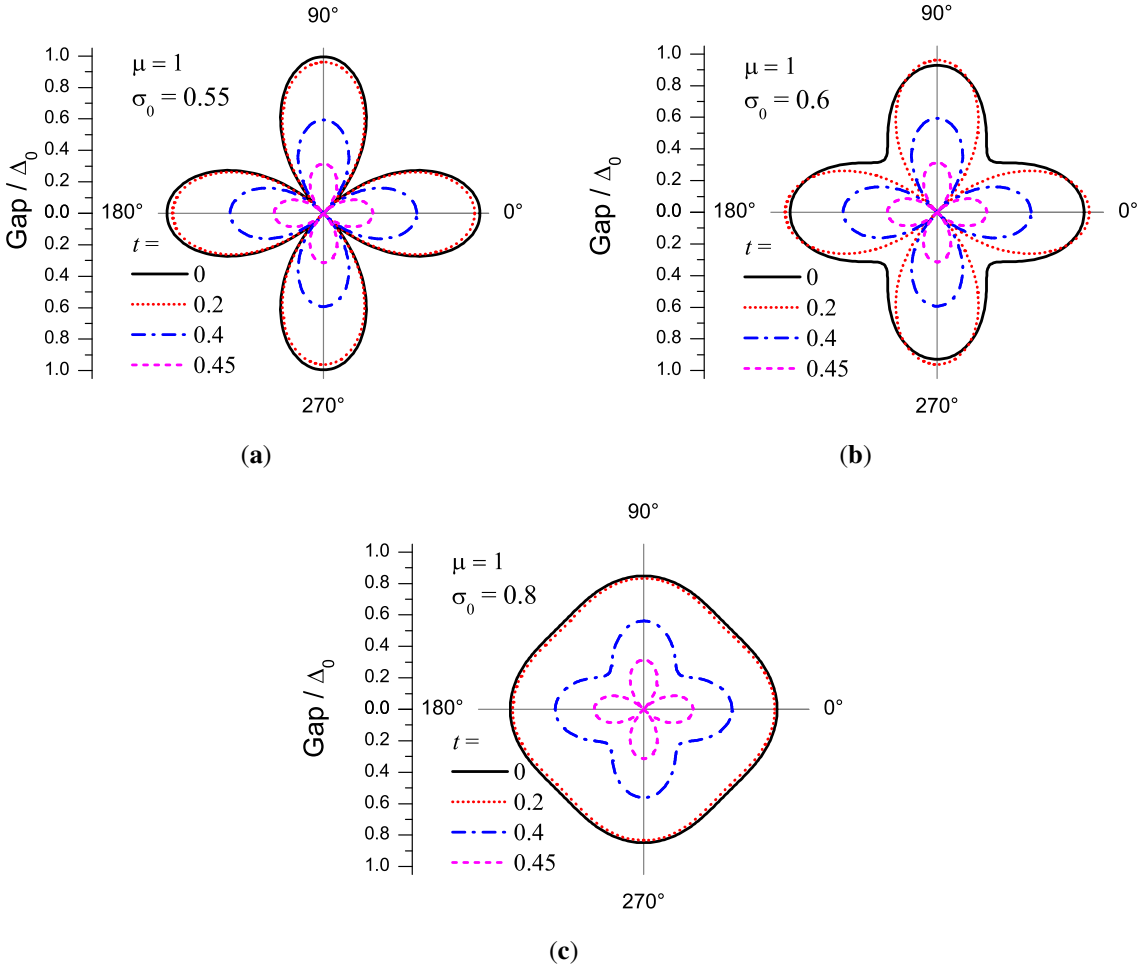

(**a**) (**b**)

(**c**)

As was indicated in Section 3, each pairing is characterized by the ratio between the zero-temperature order-parameter value and the critical temperature: R_s for s-pairing and R_d for d-one. Those ratios are notably different in partially gapped d-wave superconductors (see below and References [119–121]). The effect is even stronger for the complete dielectrization. Indeed, Figure 19 clearly demonstrates the effect in the whole range of σ_0. The calculated dependences can be explained by the examination of $\Sigma(T)$ and $\Delta(T)$ curves shown in Figure 17. Patterns for both order parameters differ substantially. Since $T_{c0} > T_{d0}$ in the whole relevant interval Equation (19), the critical temperature $T_c = T_{c0}$ is not affected by the dielectric gapping. The parameter $\Delta(0)$ rapidly decreases with σ_0, since the upper part of the $\Delta(T)$-dependence in Figure 17(b) is effectively cut away in comparison with typical theoretical or observed BCS-like curves, so that a conventional increase of $\Delta(T)$ at low T is arrested for this set of problem parameters. At the same time, $\Sigma(T)$-dependence "collapses" with decreasing σ_0 almost uniformly and similarly to T_d. As a result (see Figure 19), the ratio $\Delta(0)/T_c$ changes drastically with σ_0, whereas the ratio $\Sigma(0)/T_d$ varies insignificantly.

Figure 19. σ_0-dependences of the ratios between the order parameters at $T = 0$ and the relevant critical temperatures for complete CDW gapping.

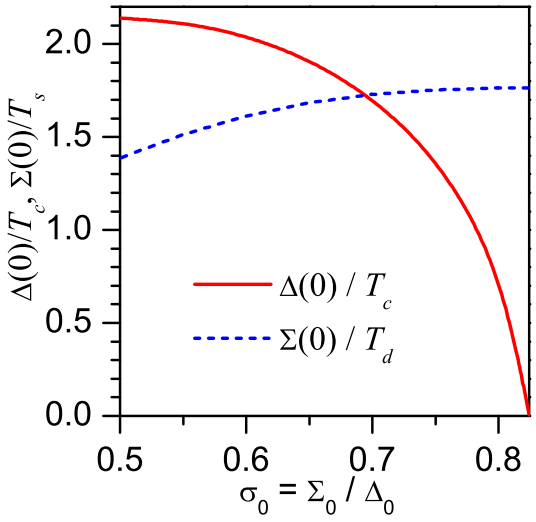

It is remarkable that in the degenerate case of complete dielectric gapping the ratio $\Delta(0)/T_c$ is always smaller than the weak-coupling d-wave BCS value R_d, whereas for the partial CDW gapping this ratio can be both larger than this weak-coupling limit, according to our theory [119] and the experiment for high-T_c oxides [134], and smaller than this limit [121]. The observed deviations in cuprates from the BCS value were interpreted earlier either as the superconductivity-driven feedback suppression of the depairing by real thermal phonons [261] or as the specific manifestation of the spin-fluctuation mechanism of Cooper pairing [262].

10. Unidirectional CDW Configuration

Let us consider now another kind of observed CDW patterns in high-T_c superconductors, with only one CDW family (stripe-like configuration) [129,130,137–140]. This configuration corresponds to the

existence of dielectric gaps only in the hatched sectors on the FS (see Figure 3). In terms of the relevant problem parameters, such a unidirectional CDW is described by the value $N = 2$ in Equation (16) and allowing α to vary from 0 to $\frac{\pi}{2}$. The range $[0, \frac{\pi}{4}]$ for the parameter β remains the same.

It is worth noting that the phase-diagram characteristic features (phase boundaries) in the checkerboard case were obtained making use of only Equation (15), which does not include N. Therefore, they remain the same at $\alpha \leq \frac{\pi}{4}$. This circumstance is illustrated in Figure 20. In particular, the lower ($0 \leq \alpha \leq \frac{\pi}{4}$) part of the phase diagram for every β in the unidirectional case reproduces the phase diagram for the checkerboard CDWs (Figure 13(a)); the upper plane ($\frac{\pi}{4} \leq \alpha \leq \frac{\pi}{2}$) is new. The figure demonstrates that no regions with T-driven CDW-reentrance exist at $\alpha \geq \frac{\pi}{4}$, since superconductivity becomes too weakened to suppress CDW gapping at low T there. On the contrary, Σ-reentrance of kind II turns more pronounced, because for any β (including *the most important* "cuprate" value $\beta = 0$), we can select such σ_0 that the variation of α would reveal the reentrance effect.

Figure 20. The same as in Figure 13(**a**), but for the unidirectional CDW configuration.

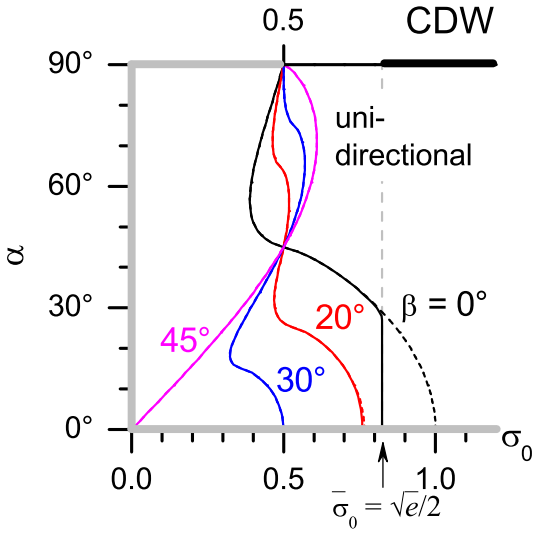

At the same time, the specific nonzero Σ- and Δ-values do differ for checkerboard and unidirectional CDW superconductors, because the N-dependent Equation (16) is to be used for their calculation. The influence of the number N of Σ-sectors on the magnitude of order parameters is illustrated in Figure 21. Here, three scenarios of the order parameter behavior are presented: one (panel a) without any reentrance, *i.e.*, the phase point is in the SC+CDW region, and other two with the reentrance in the cases $\sigma_0 > \bar{\sigma}_0$ (panel b) and $\sigma_0 < \bar{\sigma}_0$ (panel c). We can see that the value of T_c changes with N in (a) and (b) panels. It is not at all strange. Indeed, more Σ-sectors with identical opening angles correspond to a higher degree of effective FS dielectric gapping, which suppresses T_c [119]. Mathematically, it follows from the fact that T_c is determined from Equation (16), which includes the parameter N. The reciprocally detrimental effect of superconductivity and CDWs is also confirmed by the relationships between the order parameter magnitudes: in the checkerboard configuration, when the role of CDWs is higher, Σ-values are larger and Δ- values smaller than their counterparts in the unidirectional case. Additionally, the figure indicates that the phase diagram (σ_0, α)—to be more accurate, the separatrices in the (σ_0, α)-plane dividing pure-SC, SC+CDW, and CDW-reentrance phases—are independent of the Σ-sector number N at $\alpha \leq \frac{\pi}{4}$.

Figure 21. Comparison of the normalized $\Sigma(T)$- and $\Delta(T)$-dependences in the unidirectional and checkerboard configurations for various sets of system parameters.

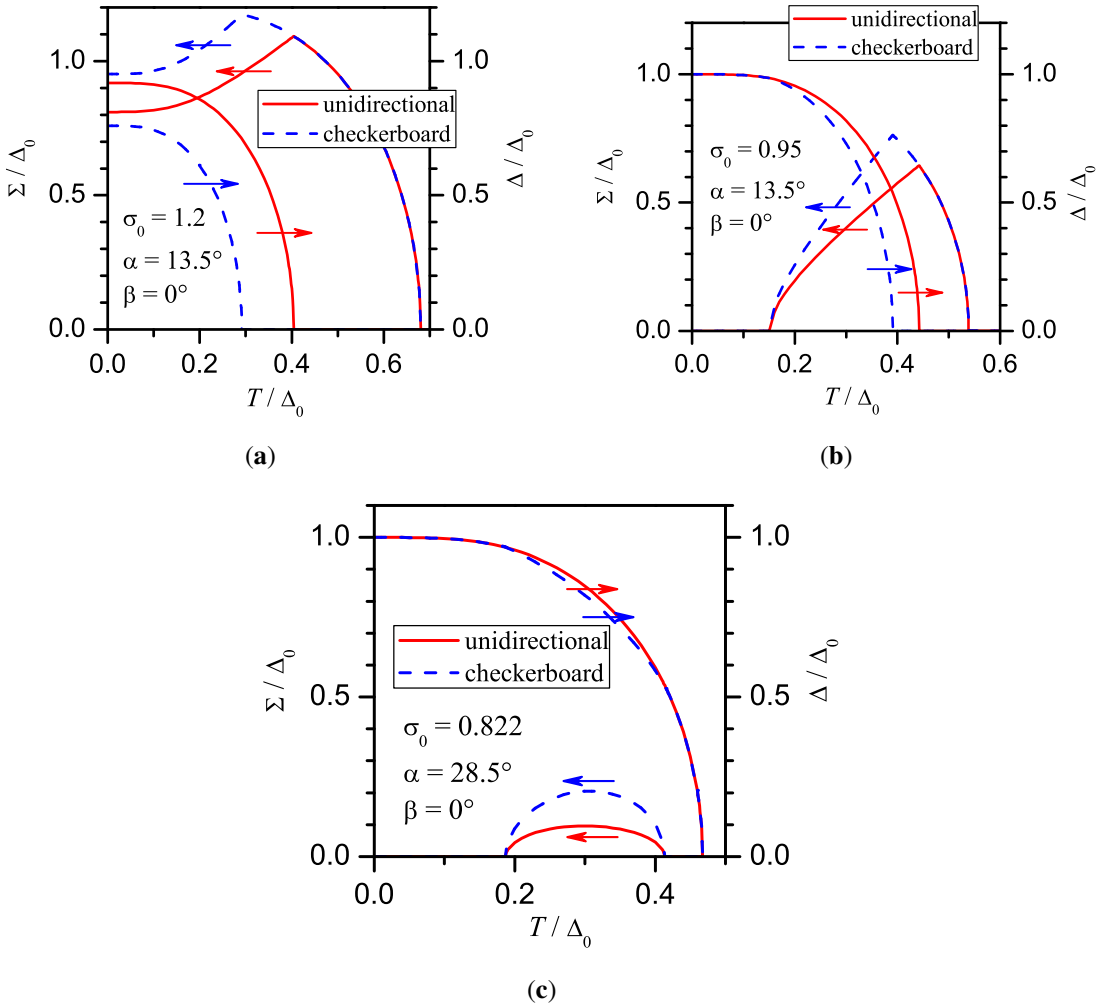

Of course, gap roses do change, sometimes drastically. In Figure 22, the temperature evolution of gap roses is exhibited for each set of problem parameters illustrated in Figure 21. The figures demonstrate that the change of Σ-sector geometry results in visibly non-similar angular gap patterns only when magnitudes of Σ and Δ are comparable. Otherwise, both roses are indistinguishable. For instance, diagrams at $t = 0.1$ and 0.45 in the checkerboard geometry are identical to their counterparts in the unidirectional one, because $\Sigma(t = 0.1) = \Sigma(t = 0.45) = 0$. At $t = 0.3$, as stems from Figure 21(c), $\Sigma(t) \neq 0$. But even in this case the difference between order parameter magnitudes in different geometries and the loss of 90°-rotation symmetry for the gap pattern are insufficient to discriminate between the checkerboard and unidirectional Σ-configurations. In particular, the gap maximum in Figure 21(a) equals 0.844, whereas two maxima in Figure 21(b) are 0.852 and 0.847 for 0°- and 90°-directions, respectively.

Figure 22. Comparison of gap-rose temperature evolution in the unidirectional and checkerboard configurations for various sets of system parameters.

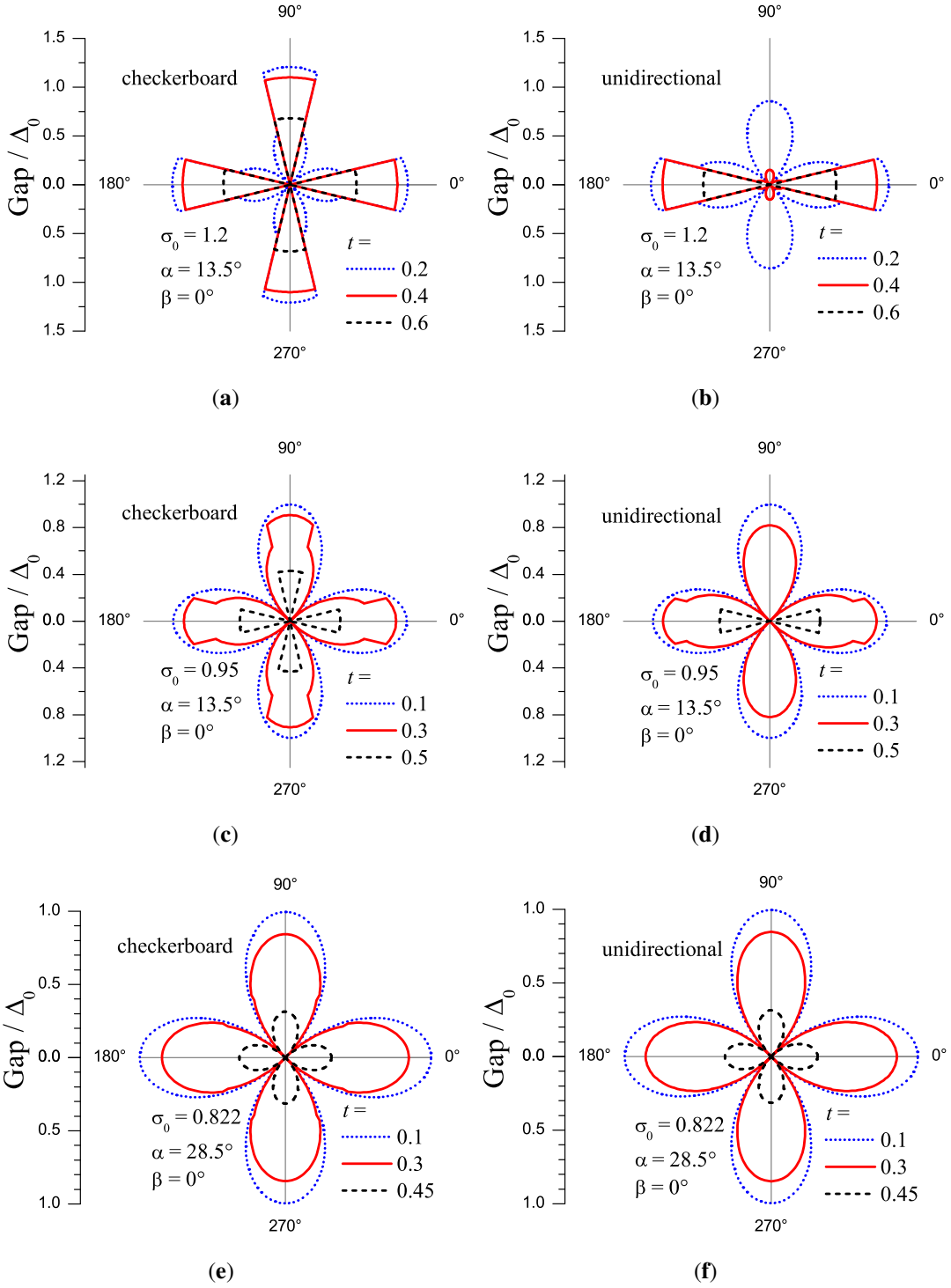

11. Ratio of the Superconducting Gap at Zero Temperature $\Delta(0)$ to the Critical Temperature T_c as an Indicator of the CDW Presence

It is well known that in the weak-coupling limit (*i.e.*, when the emergence of superconductivity does not significantly alter the underlying electron-ion background) the ratio $\Delta(0)/T_c$ is a universal constant for every specific type of the BCS-type (Cooper) pairing [24,230,231,263]. For instance, as has been mentioned above, $\Delta(0)/T_c$ equals $R_s \approx 1.764$ for the isotropic s-wave superconductor and $R_d \approx 2.140$ for the d-wave one. This remarkable universality means that the original BCS theory as well as its possible more sophisticated extensions [264] are in essence theories of corresponding states similar to the famous van der Waals theory of gases and liquids, the first of this kind [265]. In strong-coupling superconductors the universality is lost and the ratio concerned goes to depend on the gluing-boson frequency spectrum, *i.e.*, become material-specific [266].

The presented theory is a weak-coupling one for both pairings involved. Nevertheless, their interplay should change the ratios for superconducting as well as electron-hole order parameters. We are interested in the CDW influence on $\Delta(0)/T_c$, since this important quantity indicating the appearance of something unusual is often the subject of studies as well as speculations.

In Figure 23, surfaces of $\Delta(0)/T_c$ over the phase plane $\sigma_0 - \alpha$ are shown for the checkerboard CDW geometry ($N = 4$) and the distinctive cases $\beta = 0$ and $\beta = \frac{\pi}{4}$. As one can readily notice, the indicative ratio may be either larger than its inherent value R_d or smaller depending on the input parameters. It will be shown below that the larger is the increase of $\Delta(0)/T_c$, the stronger is the T_c drop under the influence of CDWs. Therefore, big experimental values of $\Delta(0)/T_c = 2.7 \div 6.5$ observed in cuprates [134,267–269] signify that their T_c may be substantially increased if one gets rid of CDWs by a due treatment of samples. Of course, this conclusion is based on the validity of our interpretation of high-T_c-oxide properties as consequences of the very CDW existence in those materials.

Figure 23. 3D-plots of the ratio $R = \Delta(0)/T_c$ on the phase plane $\alpha - \sigma_0$ for CDW (**a**) $d_{x^2-y^2}$-; and (**b**) d_{xy}-wave superconductors in the checkerboard CDW configuration.

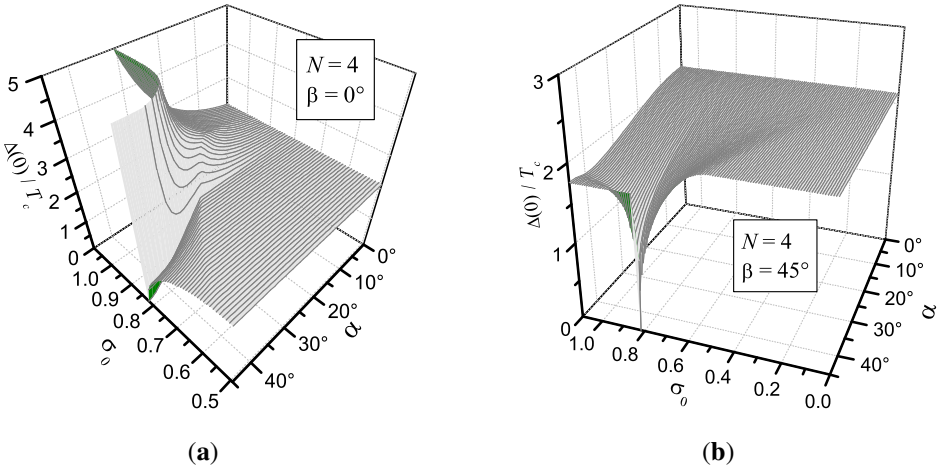

(a) **(b)**

To make the results more clear we extracted some characteristic profiles from the data presented in Figure 23. In Figure 24(a), the dependences of $2\Delta(0)/T_c$ and T_c/Δ_0 ratios on Σ_0 are shown. One sees

that $2\Delta(0)/T_c$ for $\beta = 0$ (cuprates!) sharply increases with Σ_0 for $\Sigma_0 \leq 1$ and swiftly saturates for larger Σ_0, whereas T_c/Δ_0 decreases almost evenly. The saturation value proves to be 5.2 for $\mu = 0.3$. Such a large enhancement of $\Delta(0)/T_c$ consistent with experiment *cannot* be achieved taking into account strong-coupling electron-boson interaction effects for reasonable relationships between T_c and effective boson frequencies ω_E[270,271] (one can hardly accept, e.g., the value $T_c/\omega_E \approx 0.3$ [271] as practically meaningful). Therefore, our weak-coupling model is *sufficient* to explain large $\Delta(0)/T_c$ in cuprates, possible strong-coupling effects resulting in at most minor corrections. On the other hand, with growing mismatch β between CDW-sector and superconducting lobe maxima, the ratio falls rapidly becoming not only smaller than R_d but even smaller than R_s in a certain region of the $\sigma_0 - \alpha$ phase plane (see Figure 23(b)).

Figure 24. (**a**) Dependences of the ratio $2\Delta(0)/T_c$ on σ_0 at $\mu = 0.3$ for various β; (**b**) dependences of $2\Delta(0)/T_c$ and T_c/Δ_0 on μ at $\sigma_0 = 1$ for various β.

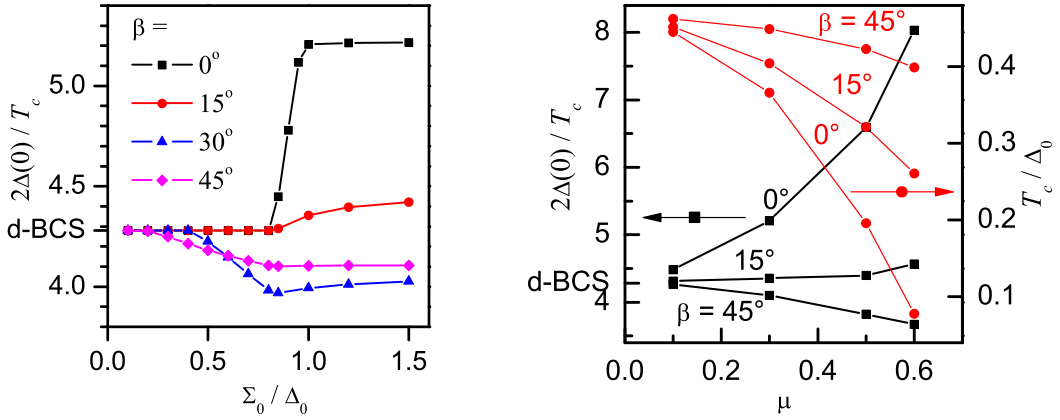

The μ-dependences of $2\Delta(0)/T_c$ and T_c/Δ_0 are shown in Figure 24(b). They confirm that $2\Delta(0)/T_c$ can reach rather large values, if the dielectric gapping sector is wide enough. This growth is however practically limited by a drastic drop of T_c leading to a quick disappearance of superconductivity. We think that it is exactly the case of underdoped cuprates, when a decrease of T_c is accompanied by a conspicuous widening of the superconducting gap. For instance, such a scenario was clearly observed in break-junction experiments for $Bi_2Sr_2CaCu_2O_{8+\delta}$ samples with a large doping range [272].

As was pointed out in Reference [134], various photoemission and tunneling measurements for different cuprate families show a typical average value $2\Delta(0)/T_c \approx 5.5$ (larger values are inherent to Hg-containing high-T_c oxides [268]). From our Figure 24(b), we see that this ratio corresponds to $\mu \approx 0.35$ at $\Sigma_0 = 1$. The other curve readily gives $T_c/\Delta_0 \approx 0.35$. Since $\Delta_0/T_{c0} \approx R_d$ for a d-wave superconductor (see above), we obtain $T_c/T_{c0} \approx 0.75$, being quite a reasonable estimation of T_c-reduction by CDWs. This justifies our conclusion made above (and many-many years ago concerning another superconducting oxide $BaPb_{1-x}Bi_xO_3$ [216]) that CDWs might be the main obstacle on the road to higher (room?) T_c's.

One can qualitatively explain the results on $\Delta(0)/T_c$ looking attentively at order parameter momentum-space configurations (Figure 3). First, consider the cuprate-related case $\beta = 0$ and the

checkerboard CDW structure. The rapid increase of the ratio $\Delta(0)/T_c$ occurs at $\sigma_0 \geq 1$ (Figure 24(a)), whereas $\Delta(0)/T_c > R_d$ for any reasonable μ (α) (Figure 24(b)). The indicated conditions correspond to a situation when $T_d > T_c$, so that CDWs suppress T_c stronger than $\Delta(0)$, when this d-wave $\Delta(T)$ grows substantially due to its steeper character in comparison with the s-wave $\Sigma(T)$ (see Figure 2).

Second, let us look at the another extreme $\beta = \frac{\pi}{4}$ with the same checkerboard-like CDWs (Figure 23(b)). Here, in a wide range of openings α and growing σ_0 (see Figure 24(a)) we arrive at the configuration when $\Delta(T \to 0)$ is more affected than T_c, the latter determined mostly by the lobe maxima. Since the node regions are effectively switched out by CDWs, superconductivity becomes almost angle-independent (momentum-independent), so that the actual $\Delta(0)/T_c$ tends to R_s, although the parent superconductivity has the d-wave symmetry!

An abyss that takes place in the vicinity of $\sigma_0 = \bar{\sigma}_0$ and at $\alpha \to \frac{\pi}{2}$ draws attention. In the whole phase diagram plane, the CDW suppress superconductivity by lowering both the $\Delta(0)$ and T_c values. But it does it nonuniformly with respect to those quantities, reducing the T_c value more effectively (see Figures 7(b) and 8(b)), so that the ratio $\Delta(0)/T_c$ grows. At the same time, in the region concerned, the CDW cannot change $T_c = T_{c0}$, but can reduce $\Delta(0)$, even down to zero, as Figure 25 demonstrates. Panel (a) of this figure testify once more that Σ has a reentrant behavior for rather large α-values in the case $N = 4$ and $\beta = 0$.

Figure 25. The same as in Figure 7, but for $\alpha = 35°$.

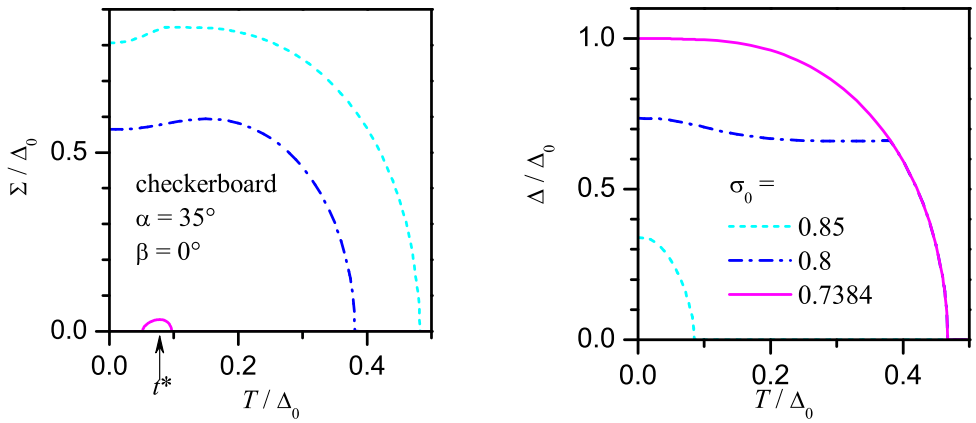

The interplay between one-dimensional stripe-like CDWs ($N = 2$) and d-wave superconductivity is quite another story (see Figure 26). In the $\beta = 0$ configuration, CDWs cannot suppress T_c stronger than $\Delta(0)$, because two superconducting lobes are CDW-free (Figure 3). Hence, typical ratios $\Delta(0)/T_c$ on the phase plane are smaller than R_d, as is shown in panel (a). On the other hand, for $N = 2$ and $\beta = \frac{\pi}{4}$ the ratios $\Delta(0)/T_c$ do not exceed R_d for small enough α, since in actual fact all lobes are equivalent and CDW-free. For $\alpha \gtrsim \frac{\pi}{4}$, the mechanism of $\Delta(0)/T_c$-increase, discussed for the configuration $N = 4$ and $\beta = 0$, starts to work (see panel (b)).

Figure 26. The same as in Figure 23, but for the unidirectional CDWs ($N = 2$).

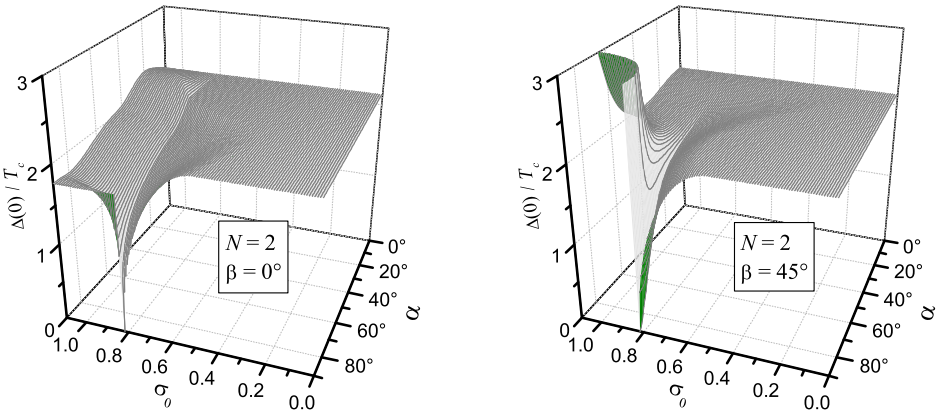

(a) **(b)**

12. Conclusions

We built a self-consistent theory of coexistence between states with different order parameter symmetry. CDWs have an s-wave symmetry, while Cooper pairing is a d-wave one. The constructed phase diagrams and various dependences of relevant quantities describing d-wave superconducting, CDW + d-wave superconducting, and reentrant CDW + d-wave superconducting phases reveal a diverse picture, being much richer than its counterpart for CDW s-wave superconductors [71]. In particular, we can draw a conclusion that the pseudogap (which we consider to be a CDW gap) in cuprates may be sometimes difficult to detect and reproduce due to its reentrant character. Hence, the calculated phase diagrams would be of help giving an important overall insight and even quantitative benchmarks. The latter is no surprise, since the control parameter α (or μ) is a measurable property [96,185,205,239], independent of fine details of the electron spectrum and being a cornerstone of the adopted phenomenological scenario.

We demonstrated that the ratio $\Delta(0)/T_c$ in CDW superconductors may differ substantially from its weak-coupling value for the parent d-wave superconductor [230,231] even if the Cooper pairing is assumed to be a weak-coupling one. This ratio may be either larger or smaller than the d-wave value R_d depending on the system parameters. For cuprates one should expect $\Delta(0)/T_c > R_d$ in agreement with the experiment [134,268].

Note, that strong Coulomb correlations between quasiparticles (Mott–Hubbard picture) [136,262,273–275] are also taken into account here although implicitly by formation of the FS with its nested and non-nested sections (hot and cold spots, respectively). Moreover, this speculative splitting is supported by the experiment [96,125,126,185,188,205,239]. We guess that the interplay between order parameters of other nature but also possessing different symmetries may lead to reentrant phenomena for the weaker order parameter, similar to that found here for $\Sigma(T)$ and $\Sigma(\alpha)$. Perhaps, some hidden interplay of this kind taking place in $Bi(Pb)_2Sr_2Ca(Tb)Cu_2O_{8+\delta}$ results in the nonmonotonic T-behavior of the pseudogap there [188].

As for strong many-body correlations between quasiparticles, it is worthwhile to mention the alternative point of view [276] attributing spatial patterns (CDWs) in various cuprates to the strong-coupling phenomena (whatever the specific scenario) rather than the nesting-driven dielectric gapping of the electron spectrum. The authors of Reference [276] found some inconsistencies in the picture supported by our analysis. For instance, they indicate that the CDW wave vectors conspicuously differ from the values dictated by the FS flat-section separation. This disagreement might be explained by Coulomb correlations (in this sense, the above-mentioned viewpoint is quite reasonable) or the actual three-dimensionality of the FS in high-T_c oxides [60]. The distinctions concerned become larger for overdoped samples, as was observed, e.g., in $Ca_{2-x}Na_xCuO_2Cl_2$. In the framework of the scenario adopted here, this is no surprise as well, since charged dopants gradually destroy both Peierls [277] and excitonic [278] insulators, leading to the CDW (and pseudogap!) disappearance in overdoped samples. At the same time, the nesting character of the FS preserves, thus reflecting the incipient instability overcome by Coulomb scatterers. Nevertheless, to be sincere, it should be indicated that nesting is only a *necessary* condition (the so-called "hidden nesting" [279] may be considered as a property closely resembling the true nesting) of the CDW ordering to take place rather than the sufficient one. Certain relevant speculations describing opposite views can be found in References [280–282].

The depicted "gap roses" show that ARPES angular diagrams represent peculiar combinations of order parameters as angle-dependent combined gaps rather than each order parameter separately (see also recent experimental data in References [100,101], as well as the analysis of photoexcited quasiparticle relaxation dynamics in Reference [98]). The same is true for tunnel and point-contact measurements, where certain tricks are used to single out each order parameter contribution [115,182,239,283]. Therefore, proportionality found between the apparent gap and temperature $T_{\rm pg}$, below which the pseudogap starts to manifests itself [284], does not mean that the observed gap is the superconducting one Δ.

Unidirectional CDWs interact with d-wave superconductivity similarly to checkerboard ones, although externally driven switch between the patterns may lead to conspicuous differences between resulting ARPES or tunnel spectra. As for a mismatch ($\beta \neq 0$) between $\Delta(\theta)$ and $\Sigma(\theta)$ maxima, it substantially changes phase diagrams. The effect would have strongly manifested itself especially for d_{xy} superconductivity if a corresponding material had been found.

Configurations with $\beta \neq 0$ and $\frac{\pi}{4}$ correspond to states that might appear in internally strained or non-hydrostatically externally pressed samples. The existence of such sample patches may explain bad reproducibility of normal-state and/or superconducting properties of high-T_c oxides.

Going beyond the specific topic of this Review, we ought to emphasize that nowadays, when the whole community celebrates the 100 anniversary of the Kamerlingh Onnes's discovery of superconductivity, one should admit that (i) "*the theory of superconductivity*" (various versions of which being depicted, e.g., in References [285–287]) does not yet exist (see discussion in References [125,126,288–295]); (ii) old failed microscopic theories of superconductivity turned out to be important steps on the long way to higher T_c's providing us with useful ingredients of the future more successful approaches [296–298]. We hope that the presented study of the role played by CDWs in high-T_c superconductors would be important for the improved understanding of the state of the art.

Acknowledgements

AMG and AIV are grateful to Kasa im. Józefa Mianowskiego, Fundacja na Rzecz Nauki Polskej, and Fundacja Zygmunta Zaleskiego for the financial support of their visits to Warsaw. MSL is grateful to the Ministry of Science and Informatics of Poland (grant No. 202-204-234). The work of AMG, AIV, MSL, and HS was partially supported by the Project N 23 of the 2009-2011 Scientific Cooperation Agreement between Poland and Ukraine. AMG highly appreciates the 2010 Visitors Program of the Max Planck Institute for the Physics of Complex Systems (Dresden, Germany). We highly appreciate interesting discussions on high-T_c superconductivity and charge-density-wave instability with S. Borisenko (Dresden), D. Evtushinsky (Dresden), D. Inosov (Stuttgart), B. Keimer (Stuttgart), J. Köhler (Stuttgart), A. Kordyuk (Dresden), D. Manske (Stuttgart), and A. Menushenkov (Moscow). More general aspects of the scientific development were discussed with V. Kuznetsov (Kiev), W. Marx (Stuttgart), and S. Vil'chinskii (Kiev).

References

1. Bickers, N.E.; Scalapino, D.J. Conserving approximations for strongly fluctuating electron systems. I. Formalism and calculational approach. *Ann. Phys.* **1989**, *193*, 206–251.
2. Li, Q.; Tsay, Y.N.; Suenaga, M.; Klemm, R.A.; Gu, G.D.; Koshizuka, N. $Bi_2Sr_2CaCu_2O_{8+\delta}$ bicrystal c-axis twist josephson junctions: A new phase-sensitive test of order parameter symmetry. *Phys. Rev. Lett.* **1999**, *83*, 4160–4163.
3. Takano, Y.; Hatano, T.; Fukuyo, A.; Ishii, A.; Ohmori, M.; Arisawa, S.; Togano, K.; Tachiki, M. d-like symmetry of the order parameter and intrinsic Josephson effects in $Bi_2Sr_2CaCu_2O_{8+\delta}$ cross-whisker junctions. *Phys. Rev. B* **2002**, *65*, 140513.
4. Latyshev, Yu.I.; Orlov, A.P.; Nikitina, A.M.; Monceau, P.; Klemm, R.A. c-axis transport in naturally grown $Bi_2Sr_2CaCu_2O_{8+\delta}$ cross-whisker junctions. *Phys. Rev. B* **2004**, *70*, 094517.
5. Klemm, R.A. The phase-sensitive c-axis twist experiments on $Bi_2Sr_2CaCu_2O_{8+\delta}$ and their implications. *Philos. Mag.* **2005**, *85*, 801–853.
6. van Harlingen, D.J. Phase-sensitive tests of the symmetry of the pairing state in the high-temperature superconductors—Evidence for $d_{x^2-y^2}$ symmetry. *Rev. Mod. Phys.* **1995**, *67*, 515–535.
7. Annett, J.F.; Goldenfeld, N.D.; Leggett, A.J. Experimental Constraints on The Pairing State of the Cuprate Superconductors: An Emerging Consensus. In *Physical Properties of High Temperature Superconductors V*; Ginsberg, D.M., Ed.; World Scientific: River Ridge, NJ, USA, 1996; pp. 375–461.
8. Tsuei, C.C.; Kirtley, J.R. Pairing symmetry in cuprate superconductors. *Rev. Mod. Phys.* **2000**, *72*, 969–1016.
9. Mannhart, J.; Chaudhari, P. High-T_c bicrystal grain boundaries. *Phys. Today* **2001**, *54*, 48–53.
10. Hilgenkamp, H.; Mannhart, J. Grain boundaries in high-T_c superconductors. *Rev. Mod. Phys.* **2002**, *74*, 485–549.
11. Tsuei, C.C.; Kirtley, J.R. Pairing Symmetry in Cuprate Superconductors: Phase-Sensitive Tests. In *The Physics of Superconductors. Vol. 1: Conventional and High-T_c Superconductors*; Bennemann, K.H., Ketterson, J.B., Eds.; Springer Verlag: Berlin, Germany, 2003; pp. 647–723.

12. Tafuri, F.; Kirtley, J.R. Weak links in high critical temperature superconductors. *Rep. Prog. Phys.* **2005**, *68*, 2573–2663.
13. Latyshev, Yu.I. Evidence for D-Wave Order Parameter Symmetry in Bi-2212 From Experiments on Interlayer Tunneling. In *Symmetry and Heterogeneity in High Temperature Superconductors*; Bianconi, A., Ed.; Springer Verlag: Dordrecht, The Netherlands, 2006; pp. 181–197.
14. Kirtley, J.R.; Tafuri, F. Tunneling Measurements of the Cuprate Superconductors. In *Handbook of High-Temperature Superconductivity. Theory and Experiment*; Schrieffer, J.R., Brooks, J.S., Eds.; Springer Verlag: New York, NY, USA, 2007; pp. 19–86.
15. Tsuei, C.C.; Kirtley, J.R. Phase-sensitive tests of pairing symmetry in cuprate superconductors. In *Superconductivity. Vol. 2: Novel Superconductors*; Bennemann, K.H., Ketterson, J.B., Eds.; Springer Verlag: Berlin, Germany, 2008; pp. 869–921.
16. Prozorov, R. Superfluid density in a superconductor with an extended d-wave gap. *Supercond. Sci. Technol.* **2008**, *21*, 082003.
17. Zhao, G.-M. Identification of the bulk pairing symmetry in high-temperature superconductors: Evidence for an extended s wave with eight line nodes. *Phys. Rev. B* **2001**, *64*, 024503:1–024503:10.
18. Brandow, B.H. Arguments and evidence for a node-containing anisotropic *s*-wave gap form in the cuprate superconductors. *Phys. Rev. B* **2002**, *65*, 054503.
19. Brandow, B.H. Strongly anisotropic *s*-wave gaps in exotic superconductors. *Philos. Mag.* **2003**, *83*, 2487–2519.
20. Zhao, G.M. Unambiguous evidence for extended s-wave pairing symmetry in hole-doped high-temperature superconductors. *Philos. Mag. B* **2004**, *84*, 3861–3867.
21. Zhao, G.M. The magnetic resonance in high-temperature superconductors: Evidence for an extended s-wave pairing symmetry. *Philos. Mag. B* **2004**, *84*, 3869–3882.
22. Zhao, G.M. Precise determination of the superconducting gap along the diagonal direction of $Bi_2Sr_2CaCu_2O_{8+y}$: Evidence for an extended s-wave gap symmetry. *Phys. Rev. B* **2007**, *75*, 140510.
23. Annett, J.F. Symmetry of the order parameter for high-temperature superconductivity. *Adv. Phys.* **1990**, *39*, 83–126.
24. Mineev, V.P.; Samokhin, K.V. *Intoduction to Unconventional Superconductivity*; Gordon and Breach Science Publishers: Amsterdam, The Netherlands, 1999.
25. Gabovich, A.M.; Voitenko, A.I. Power-law low-temperature asymptotics for spatially nonhomogeneous *s*-wave superconductors. *Fiz. Nizk. Temp.* **1999**, *25*, 677–684.
26. Gabovich, A.M.; Voitenko, A.I. Influence of the order parameter nonhomogeneities on low-temperature properties of superconductors. *Phys. Rev. B* **1999**, *60*, 7465–7472.
27. Gabovich, A.M.; Li, M.S.; Szymczak, H.; Voitenko, A.I. Heat capacity of mesoscopically disordered superconductors: Implications to MgB_2. *Fiz. Nizk. Temp.* **2002**, *28*, 1126–1137.
28. Gabovich, A.M.; Li, M.S.; Pękała, M.; Szymczak, H.; Voitenko, A.I. Heat capacity of mesoscopically disordered superconductors with emphasis on MgB_2. *J. Phys. Condens. Matter* **2002**, *14*, 9621–9629.

29. Ekino, T.; Gabovich, A.M.; Li, M.S.; Takasaki, T.; Voitenko, A.I.; Akimitsu, J.; Fujii, H.; Muranaka, T.; Pękała, M.; Szymczak, H. Spatially heterogeneous character of superconductivity in MgB_2 as revealed by local probe and bulk measurements. *Physica C* **2005**, *426-431*, 230–233.
30. Phillips, J.C. States in the superconductive energy gap of high-T_c cuprates. *Phys. Rev. B* **1990**, *41*, 8968–8973.
31. Phillips, J.C. Dopant sites and structure in high T_c layered cuprates. *Philos. Mag. B* **1999**, *79*, 1477–1498.
32. Phillips, J.C.; Saxena, A.; Bishop, A.R. Pseudogaps, dopants, and strong disorder in cuprate high-temperature superconductors. *Rep. Prog. Phys.* **2003**, *66*, 2111–2182.
33. Phillips, J.C. Hard-wired dopant networks and the prediction of high transition temperatures in ceramic superconductors. *J. Supercond.* **2010**, *23*, 1267–1279.
34. Gavrilkin, S.Yu.; Ivanenko, O.M.; Martovitskii, V.P.; Mitsen, K.V.; Tsvetkov, A.Yu. Percolative nature of the transition from 60 to 90 K-phase in $YBa_2Cu_3O_{6+\delta}$. *Physica C* **2010**, *470*, S996–S997.
35. Khasanov, R.; Shengelaya, A.; Maisuradze, A.; Di Castro, D.; Savić, I.M.; Weyeneth, S.; Park, M.S.; Jang, D.J.; Lee, S.-I.; Keller, H. Nodeless superconductivity in the infinite-layer electron-doped cuprate superconductor $Sr_{0.9}La_{0.1}CuO_2$. *Phys. Rev. B* **2008**, *77*, 184512.
36. Valli, A.; Sangiovanni, G.; Capone, M.; Di Castro, C. Possible secondary component of the order parameter observed in London penetration depth measurements. *Phys. Rev. B* **2010**, *82*, 132504.
37. Buzdin, A.I.; Bulaevskii, L.N.; Kulic, M.L.; Panyukov, S.V. Magnetic superconductors. *Usp. Fiz. Nauk* **1984**, *144*, 597–641.
38. Machida, K. Coexistence problem of magnetism and superconductivity. *Appl. Phys. A* **1984**, *35*, 193–215.
39. Buzdin, A.I.; Bulaevskii, L.N. Antiferromagnetic superconductors. *Usp. Fiz. Nauk* **1986**, *149*, 45–67.
40. Bulaevskii, L.N.; Buzdin, A.I.; Kulić, M.L.; Panjukov, S.V. Coexistence of superconductivity and magnetism. Theoretical predictions and experimental results. *Adv. Phys.* **1985**, *34*, 175–261.
41. Izyumov, Yu.A.; Katsnelson, M.I.; Skryabin, Yu.N. *Itinerant Electron Magnetism*; Fiziko-Matematicheskaya Literatura: Moscow, Russia, 1994; p. 368. in Russian.
42. Santini, P.; Lémanski, R.; Erdös, P. Magnetism of actinide compounds. *Adv. Phys.* **1999**, *48*, 537–653.
43. Müller, K.-H.; Narozhnyi, V.N. Interaction of superconductivity and magnetism in borocarbide superconductors. *Rep. Prog. Phys.* **2001**, *64*, 943–1008.
44. Klamut, P.W. Superconductivity and magnetism in the ruthenocuprates. *Supercond. Sci. Technol.* **2008**, *21*, 093001.
45. Pfleiderer, C. Superconducting phases of f-electron compounds. *Rev. Mod. Phys.* **2009**, *81*, 1551–1624.
46. Moore, K.T.; van der Laan, G. Nature of the $5f$ states in actinide metals. *Rev. Mod. Phys.* **2009**, *81*, 235–298.
47. Johnston, D.C. The puzzle of high temperature superconductivity in layered iron pnictides and chalcogenides. *Adv. Phys.* **2010**, *59*, 803–1061.

48. Lumsden, M.D.; Christianson, A.D. Magnetism in Fe-based superconductors. *J. Phys. Condens. Matter* **2010**, *22*, 203203.
49. Fawcett, E.; Alberts, H.L.; Galkin, V.Yu.; Noakes, D.R.; Yakhmi, J.V. Spin-density-wave antiferromagnetism in chromium alloys. *Rev. Mod. Phys.* **1994**, *66*, 25–127.
50. Gabovich, A.M.; Voitenko, A.I. Superconductors with charge- and spin-density waves: Theory and experiment (Review). *Fiz. Nizk. Temp.* **2000**, *26*, 419–452.
51. Gabovich, A.M.; Voitenko, A.I.; Annett, J.F.; Ausloos, M. Charge- and spin-density-wave superconductors. *Supercond. Sci. Technol.* **2001**, *14*, R1–R27.
52. Gabovich, A.M.; Voitenko, A.I.; Ausloos, M. Charge-density waves and spin-density waves in existing superconductors: Competition between Cooper pairing and Peierls or excitonic instabilities. *Phys. Rep.* **2002**, *367*, 583–709.
53. Jérome, D.; Pasquier, C.R. One Dimensional Organic Superconductors. In *Frontiers in Superconducting Materials*; Narlikar, A.V., Ed.; Springer Verlag: New York, NY, USA, 2005; pp. 183–230.
54. Zhang, W.; de Melo, C.A.R.S. Triplet versus singlet superconductivity in quasi-one-dimensional conductors. *Adv. Phys.* **2007**, *56*, 545–652.
55. Aperis, A.; Varelogiannis, G.; Littlewood, P.B.; Simons, B.D. Coexistence of spin density wave, d-wave singlet and staggered π-triplet superconductivity. *J. Phys. Condens. Matter* **2008**, *20*, 434235.
56. Vojta, M. Lattice symmetry breaking in cuprate superconductors: Stripes, nematics, and superconductivity. *Adv. Phys.* **2009**, *58*, 699–820.
57. Gabovich, A.M.; Voitenko, A.I. Superconductivity against dielecrization: Evidence for competition and coexistence. *Ukr. Fiz. Zh.* **1999**, *44*, 223–229.
58. Kusmartsev, F.V.; Saarela, M. Two-component physics of cuprates and superconductor-insulator transitions. *Supercond. Sci. Technol.* **2008**, *22*, 014008.
59. Kusmartsev, F.V.; Saarela, M. What is the most important for a nanoscale structure formations in HTSC?, spin, phonon or third way in Coulomb interaction and correlations? *J. Phys. Conf. Ser.* **2008**, *108*, 012029.
60. Gabovich, A.M.; Voitenko, A.I.; Ekino, T.; Li, M.S.; Szymczak, H.; Pękała, M. Competition of superconductivity and charge density waves in cuprates: Recent evidence and interpretation. *Adv. Condens. Matter Phys.* **2010**, *2010*, 681070.
61. Bilbro, G.; McMillan, W.L. Theoretical model of superconductivity and the martensitic transformation in A15 compounds. *Phys. Rev. B* **1976**, *14*, 1887–1892.
62. Balseiro, C.A.; Falicov, L.M. Superconductivity and charge-density waves. *Phys. Rev. B* **1979**, *20*, 4457–4464.
63. Gabovich, A.M.; Pashitskii, E.A.; Shpigel, A.S. Paramagnetic limit of superconductors with a dielectric gap on the Fermi surface. *Zh. Éksp. Teor. Fiz.* **1979**, *77*, 1157–1166.
64. Gabovich, A.M.; Moiseev, D.P.; Shpigel, A.S. Thermodynamic properties of superconducting ceramics $BaPb_{1-x}Bi_xO_3$. *J. Phys. C* **1982**, *15*, L569–L572.

65. Gabovich, A.M.; Moiseev, D.P.; Shpigel, A.S. The nature of superconductivity for solid solutions $BaPb_{1-x}Bi_xO_3$ with a perovskite structure. Role of the electron spectrum dielectrization. *Zh. Éksp. Teor. Fiz.* **1982**, *83*, 1383–1388.
66. Gabovich, A.M.; Shpigel, A.S. Influence of impurity scattering on the critical temperature of superconductors with a partial gap in the electron spectrum. *J. Low Temp. Phys.* **1983**, *51*, 581–599.
67. Gabovich, A.M.; Moiseev, D.P.; Prokopovich, L.V.; Uvarova, S.K.; Yachmenev, V.E. Experimental proof of bulk superconductivity in perovskite system $BaPb_{1-x}Bi_xO_3$. *Zh. Éksp. Teor. Fiz.* **1984**, *86*, 1727–1733.
68. Gabovich, A.M.; Shpigel, A.S. Thermodynamics of superconductors with charge- and spin-density waves. *J. Phys. F* **1984**, *14*, 3031–3039.
69. Gabovich, A.M.; Gerber, A.S.; Shpigel, A.S. Thermodynamics of superconductors with charge- and spin-density waves. Δ/T_c ratio and paramagnetic limit. *Phys. Status Solidi B* **1987**, *141*, 575–587.
70. Gabovich, A.M.; Shpigel, A.S. Upper critical magnetic field of superconductors with a dielectric gap on the Fermi surface sections. *Phys. Rev. B* **1988**, *38*, 297–306.
71. Gabovich, A.M.; Li, M.S.; Szymczak, H.; Voitenko, A.I. Thermodynamics of superconductors with charge-density waves. *J. Phys. Condens. Matter* **2003**, *15*, 2745–2753.
72. Gabovich, A.M.; Voitenko, A.I.; Ekino, T. Enhanced paramagnetic limit of the upper critical magnetic field for superconductors with charge-density waves. *J. Phys. Condens. Matter* **2004**, *16*, 3681–3690.
73. Ekino, T.; Gabovich, A.M.; Voitenko, A.I. Paramagnetic effect of the magnetic field on superconductors with charge-density waves. *Fiz. Nizk. Temp.* **2005**, *31*, 55–62.
74. Gabovich, A.M. Josephson and quasiparticle tunneling in superconductors with charge density waves. *Fiz. Nizk. Temp.* **1992**, *18*, 693–704.
75. Gabovich, A.M. Josephson and quasiparticle current in partially-dielectrized superconductors with spin density waves. *Fiz. Nizk. Temp.* **1993**, *19*, 641–654.
76. Gabovich, A.M. About tunnel spectroscopy of normal metals with charge or spin density waves. *Fiz. Nizk. Temp.* **1993**, *19*, 1098–1105.
77. Gabovich, A.M.; Voitenko, A.I. Tunneling spectroscopy of normal metals with charge-density or spin-density waves. *Phys. Rev. B* **1995**, *52*, 7437–7447.
78. Gabovich, A.M.; Voitenko, A.I. Non-stationary Josephson effect for superconductors with charge-density waves: $NbSe_3$. *Europhys. Lett.* **1997**, *38*, 371–376.
79. Gabovich, A.M.; Voitenko, A.I. Nonstationary Josephson effect for superconductors with charge-density waves. *Phys. Rev. B* **1997**, *55*, 1081–1099.
80. Gabovich, A.M.; Voitenko, A.I. Josephson tunnelling involving superconductors with charge-density waves. *J. Phys. Condens. Matter* **1997**, *9*, 3901–3920.
81. Gabovich, A.M.; Voitenko, A.I. Asymmetrical tunneling between similar metallic junctions with charge-density or spin-density waves: The case of broken symmetry. *Phys. Rev. B* **1997**, *56*, 7785–7788.

82. Gabovich, A.M.; Voitenko, A.I. Nonstationary Josephson effect for superconductors with spin-density waves. *Phys. Rev. B* **1999**, *60*, 14897–14906.
83. Gabovich, A.M.; Voitenko, A.I. Nonstationary Josephson tunneling involving superconductors with spin-density waves. *Physica C* **2000**, *329*, 198–230.
84. Gabovich, A.M.; Voitenko, A.I. Charge-density-wave origin of the dip-hump structure in tunnel spectra of the BSCCO superconductor. *Phys. Rev. B* **2007**, *75*, 064516.
85. Ekino, T.; Gabovich, A.M.; Li, M.S.; Pękała, M.; Szymczak, H.; Voitenko, A.I. Analysis of the pseudogap-related structure in tunneling spectra of superconducting $Bi_2Sr_2CaCu_2O_{8+\delta}$ revealed by the break-junction technique. *Phys. Rev. B* **2007**, *76*, 180503.
86. Ekino, T.; Gabovich, A.M.; Li, M.S.; Pękała, M.; Szymczak, H.; Voitenko, A.I. Temperature-dependent pseudogap-like features in tunnel spectra of high-T_c cuprates as a manifestation of charge-density waves. *J. Phys. Condens. Matter* **2008**, *20*, 425218.
87. Morosan, E.; Wagner, K.E.; Zhao, L.L.; Hor, Y.; Williams, A.J.; Tao, J.; Zhu, Y.; Cava, R.J. Multiple electronic transitions and superconductivity in Pd_xTiSe_2. *Phys. Rev. B* **2010**, *81*, 094524.
88. Monney, C.; Schwier, E.F.; Garnier, M.G.; Mariotti, N.; Didiot, C.; Cercellier, H.; Marcus, J.; Berger, H.; Beck, A.N.T.H.; Aebi, P. Probing the exciton condensate phase in $1T$-$TiSe_2$ with photoemission. *New J. Phys.* **2010**, *12*, 125019.
89. Kudo, K.; Nishikubo, Y.; Nohara, M. Coexistence of superconductivity and charge density wave in $SrPt_2As_2$. *J. Phys. Soc. Jpn.* **2008**, *79*, 123710.
90. van Wezel, J.; Nahai-Williamson, P.; Saxena, S.S. An alternative interpretation of recent ARPES measurements on $TiSe_2$. *Europhys. Lett.* **2010**, *89*, 47004.
91. Ge, Y.; Liu, A.Y. First-principles investigation of the charge-density-wave instability in $1T$-$TaSe_2$. *Phys. Rev. B* **2010**, *82*, 155133.
92. Li, L.J.; Sun, Y.P.; Zhu, X.D.; Wang, B.S.; Zhu, X.B.; Yang, Z.R.; Song, W.H. Growth and superconductivity of $2H$-$Ni_{0.02}TaSe_2$ single crystals. *Solid State Commun.* **2010**, *150*, 2248–2252.
93. Markiewicz, R.S. A survey of the Van Hove scenario for high-T_c superconductivity with special emphasis on pseudogaps and striped phases. *J. Phys. Chem. Solids* **1997**, *58*, 1179–1310.
94. Fujita, M.; Goka, H.; Yamada, K.; Tranquada, J.M.; Regnault, L.P. Stripe order, depinning, and fluctuations in $La_{1.875}Ba_{0.125}CuO_4$ and $La_{1.875}Ba_{0.075}Sr_{0.050}CuO_4$. *Phys. Rev. B* **2004**, *70*, 104517.
95. Meevasana, W.; Ingle, N.J.C.; Lu, D.H.; Shi, J.R.; Baumberger, F.; Shen, K.M.; Lee, W.S.; Cuk, T.; Eisaki, H.; Devereaux, T.P.; Nagaosa, N.; Zaanen, J.; Shen, Z.-X. Doping dependence of the coupling of electrons to bosonic modes in the single-layer high-temperature $Bi_2Sr_2CuO_6$ superconductor. *Phys. Rev. Lett.* **2006**, *96*, 157003.
96. Lee, W.S.; Vishik, I.M.; Tanaka, K.; Lu, D.H.; Sasagawa, T.; Nagaosa, N.; Devereaux, T.P.; Hussain, Z.; Shen, Z.-X. Abrupt onset of a second energy gap at the superconducting transition of underdoped Bi2212. *Nature* **2007**, *450*, 81–84.

97. Wise, W.D.; Boyer, M.C.; Chatterjee, K.; Kondo, T.; Takeuchi, T.; Ikuta, H.; Wang, Y.; Hudson, E.W. Charge-density-wave origin of cuprate checkerboard visualized by scanning tunnelling microscopy. *Nat. Phys.* **2008**, *4*, 696–699.
98. Nair, S.K.; Zou, X.; Chia, E.E.M.; Zhu, J.-X.; Panagopoulos, C.; Ishida, S.; Uchida, S. Quasiparticle dynamics in overdoped $Bi_{1.4}Pb_{0.7}Sr_{1.9}CaCu_2O_{8+\delta}$: Coexistence of superconducting gap and pseudogap below T_c. *Phys. Rev. B* **2010**, *82*, 212503.
99. Razzoli, E.; Sassa, Y.; Drachuck, G.; Månsson, M.; Keren, A.; Shay, M.; Berntsen, M.H.; Tjernberg, O.; Radovic, M.; Chang, J.; *et al.* The Fermi surface and band folding in $La_{2-x}Sr_xCuO_4$, probed by angle-resolved photoemission. *New J. Phys.* **2010**, *12*, 125003.
100. Vishik, I.M.; Lee, W.S.; He, R.-H.; Hashimoto, M.; Hussain, Z.; Devereaux, T.P.; Shen, Z.-X. ARPES studies of cuprate Fermiology: Superconductivity, pseudogap and quasiparticle dynamics. *New J. Phys.* **2010**, *12*, 105008.
101. Kondo, T.; Hamaya, Y.; Palczewski, A.D.; Takeuchi, T.; Wen, J.S.; Xu, Z.J.; Gu, G.; Schmalian, J.; Kaminski, A. Disentangling Cooper-pair formation above the transition temperature from the pseudogap state in the cuprates. *Nat. Phys.* **2011**, *7*, 21–25.
102. Furrer, A. Admixture of an s-Wave Component to the d-Wave Gap Symmetry In High-Temperature Superconductors. In *High T_c Superconductors and Related Transition Metal Oxides. Special Contributions in Honor of K. Alex Müller on the Occasion of his 80th Birthday*; Bussmann-Holder, A., Keller, H., Eds.; Springer Verlag: Heidelberg, Germany, 2007; pp. 135–141.
103. Cohen, M.L. Essay: Fifty years of condensed matter physics. *Phys. Rev. Lett.* **2008**, *101*, 250001.
104. Burgin, M.S.; Kuznetsov, V.I. Scientific problems and questions from a logical point of view. *Synthese* **1994**, *100*, 1–28.
105. Popper, K.R. *Objective Knowledge. An Evolutionary Approach*; Clarendon Press: Oxford, UK, 1979.
106. Krasnov, V.M.; Yurgens, A.; Winkler, D.; Delsing, P.; Claeson, T. Evidence for coexistence of the superconducting gap and the pseudogap in Bi-2212 from intrinsic tunneling spectroscopy. *Phys. Rev. Lett.* **2000**, *84*, 5860–5863.
107. Oda, M.; Liu, Y.H.; Kurosawa, T.; Takeyama, K.; Momono, N.; Ido, M. On the relations among the pseudogap, electronic charge order and Fermi-arc superconductivity in $Bi_2Sr_2CaCu_2O_{8+\delta}$. *J. Phys. Conf. Ser.* **2008**, *108*, 012008.
108. Li, Y.; Balédent, V.; Yu, G.; Barišić, N.; Hradil, K.; Mole, R.A.; Sidis, Y.; Steffens, P.; Zhao, X.; Bourges, P.; Greven, M. Hidden magnetic excitation in the pseudogap phase of a high-T_c superconductor. *Nature* **2010**, *468*, 283–285.
109. Parker, C.V.; Aynajian, P.; da Silva Neto, E.H.; Pushp, A.; Ono, S.; Wen, J.; Xu, Z.; Gu, G.; Yazdani, A. Fluctuating stripes at the onset of the pseudogap in the high-T_c superconductor $Bi_2Sr_2CaCu_2O_{8+x}$. *Nature* **2010**, *468*, 677–680.
110. Kudo, K.; Nishizaki, T.; Okamoto, D.; Okumura, N.; Kobayashi, N. STM/STS studies on the energy gap of Pb-substituted $Bi_2Sr_2CuO_{6+\delta}$ in magnetic fields. *Physica C* **2010**, *470*, S195–S196.
111. van der Marel, D. Beware of the pseudogap. *Nat. Phys.* **2011**, *7*, 10–11.

112. He, R.-H.; Hashimoto, M.; Karapetyan, H.; Koralek, J.D.; Hinton, J.P.; Testaud, J.P.; Nathan, V.; Yoshida, Y.; Yao, H.; Tanaka, K.; *et al.* From a single-band metal to a high-temperature superconductor via two thermal phase transitions. *Science* **2011**, *331*, 1579–1583.
113. Lee, J.; Fujita, K.; McElroy, K.; Slezak, J.A.; Wang, M.; Aiura, Y.; Bando, H.; Ishikado, M.; Masui, T.; Zhu, J.-X.; Balatsky, A.V.; Eisaki, H.; Uchida, S.; Davis, J.C. Interplay of electron-lattice interactions and superconductivity in $Bi_2Sr_2CaCu_2O_{8+\delta}$. *Nature* **2006**, *442*, 546–551.
114. Reznik, D.; Pintschovius, L.; Ito, M.; Iikubo, S.; Sato, M.; Goka, H.; Fujita, M.; Yamada, K.; Gu, G.D.; Tranquada, J.M. Electron-phonon coupling reflecting dynamic charge inhomogeneity in copper oxide superconductors. *Nature* **2006**, *440*, 1170–1173.
115. Boyer, M.C.; Wise, W.D.; Chatterjee, K.; Yi, M.; Kondo, T.; Takeuchi, T.; Ikuta, H.; Hudson, E.W. Imaging the two gaps of the high-temperature superconductor $Bi_2Sr_2CuO_{6+x}$. *Nat. Phys.* **2007**, *3*, 802–806.
116. Yazdani, A. Visualizing pair formation on the atomic scale and the search for the mechanism of superconductivity in high-T_c cuprates. *J. Phys. Condens. Matter* **2009**, *21*, 164214.
117. Kato, T.; Machida, T.; Kamijo, Y.; Miyashita, R.; Sakata, H. Spatial correlation between the LDOS modulation and electronic inhomogeneity in $Bi_2Sr_{2-x}La_xCuO_{6+\delta}$. *J. Phys. Conf. Ser.* **2009**, *150*, 052101.
118. Parker, C.V.; Pushp, A.; Pasupathy, A.N.; Gomes, K.K.; Wen, J.; Xu, Z.; Ono, S.; Gu, G.; Yazdani, A. Nanoscale proximity effect in the high-temperature superconductor $Bi_2Sr_2CaCu_2O_{8+\delta}$ using a scanning tunneling microscope. *Phys. Rev. Lett.* **2010**, *104*, 117001.
119. Gabovich, A.M.; Voitenko, A.I. Model for the coexistence of d-wave superconducting and charge-density-wave order parameters in high-temperature cuprate superconductors. *Phys. Rev. B* **2009**, *80*, 224501.
120. Voitenko, A.I.; Gabovich, A.M. Charge-density waves in partially dielectrized superconductors with d-pairing. *Fiz. Tverd. Tela* **2010**, *52*, 20–27.
121. Voitenko, A.I.; Gabovich, A.M. Charge density waves in d-wave superconductors. *Fiz. Nizk. Temp.* **2010**, *36*, 1300–1311.
122. Friend, R.H.; Jérome, D. Periodic lattice distortions and charge-density waves in one-dimensional and 2-dimensional metals. *J. Phys. C* **1979**, *12*, 1441–1477.
123. Friend, R.H.; Yoffe, A.D. Electronic properties of intercalation complexes of the transition metal dichalcogenides. *Adv. Phys.* **1987**, *36*, 1–94.
124. Vojta, M. Tendencies toward nematic order in $YBa_2Cu_3O_{6+\delta}$: Uniform distortion vs. incipient charge stripes. *Eur. Phys. J. Spec. Top.* **2010**, *188*, 49–59.
125. Kordyuk, A.A.; Zabolotnyy, V.B.; Evtushinsky, D.V.; Büchner, B.; Borisenko, S.V. Electrons in cuprates: A consistent ARPES view. *J. Electron Spectrosc. Relat. Phenom.* **2010**, *181*, 44–47.
126. Kordyuk, A.A.; Zabolotnyy, V.B.; Evtushinsky, D.V.; Inosov, D.S.; Kim, T.K.; Büchner, B.; Borisenko, S.V. An ARPES view on the high-T_c problem: Phonons vs. spin-fluctuations. *Eur. Phys. J. Spec. Top.* **2010**, *188*, 153–162.
127. Franz, M. Crystalline electron pairs. *Science* **2004**, *305*, 1410–1411.

128. McElroy, K.; Lee, D.-H.; Hoffman, J.E.; Lang, K.M.; Lee, J.; Hudson, E.W.; Eisaki, H.; Uchida, S.; Davis, J.C. Coincidence of checkerboard charge order and antinodal state decoherence in strongly underdoped superconducting $Bi_2Sr_2CaCu_2O_{8+\delta}$. *Phys. Rev. Lett.* **2005**, *94*, 197005.
129. Robertson, J.A.; Kivelson, S.A.; Fradkin, E.; Fang, A.C.; Kapitulnik, A. Distinguishing patterns of charge order: Stripes or checkerboards. *Phys. Rev. B* **2006**, *74*, 134507.
130. Del Maestro, A.; Rosenow, B.; Sachdev, S. From stripe to checkerboard ordering of charge-density waves on the square lattice in the presence of quenched disorder. *Phys. Rev. B* **2006**, *74*, 024520.
131. Wróbel, P. Checkerboard or stripes: Hard-core bosons on the checkerboard lattice as a model of charge ordering in planar cuprates. *Phys. Rev. B* **2006**, *74*, 014507.
132. Zhao, H.-W.; Zha, G.-Q.; Zhou, S.-P. Checkerboard-pattern vortex with the long-range Coulomb interaction in underdoped high-temperature superconductors. *New J. Phys.* **2008**, *10*, 043047.
133. Annett, J.F. Unconventional superconductivity. *Contemp. Phys.* **1995**, *36*, 423–437.
134. Damascelli, A.; Hussain, Z.; Shen, Z.-X. Angle-resolved photoemission studies of the cuprate superconductors. *Rev. Mod. Phys.* **2003**, *75*, 473–541.
135. Markiewicz, R.S. STM checkerboards from crossed stripes: A static stripe model. *Phys. Rev. B* **2005**, *71*, 220504.
136. Lee, P.A. From high temperature superconductivity to quantum spin liquid: Progress in strong correlation physics. *Rep. Prog. Phys.* **2008**, *71*, 012501.
137. Tranquada, J.M.; Sternlieb, B.J.; Axe, J.D.; Nakamura, Y.; Uchida, S. Evidence for stripe correlations of spins and holes in copper oxide superconductors. *Nature* **1995**, *375*, 561–563.
138. Zachar, O.; Kivelson, S.A.; Emery, V.J. Landau theory of stripe phases in cuprates and nickelates. *Phys. Rev. B* **1998**, *57*, 1422–1426.
139. Caprara, S.; Castellani, C.; Di Castro, C.; Grilli, M.; Perali, A. Charge and spin inhomogeneity as a key to the physics of the high-T_c cuprates. *Physica B* **2000**, *280*, 196–200.
140. Kohsaka, Y.; Taylor, C.; Fujita, K.; Schmidt, A.; Lupien, C.; Hanaguri, T.; Azuma, M.; Takano, M.; Eisaki, H.; Takagi, H.; Uchida, S.; Davis, J.C. An intrinsic bond-centered electronic glass with unidirectional domains in underdoped cuprates. *Science* **2007**, *315*, 1380–1385.
141. Kivelson, S.A.; Bindloss, I.P.; Fradkin, E.; Oganesyan, V.; Tranquada, J.M.; Kapitulnik, A.; Howald, C. How to detect fluctuating stripes in the high-temperature superconductors. *Rev. Mod. Phys.* **2003**, *75*, 1201–1241.
142. Daou, R.; Chang, J.; LeBoeuf, D.; Cyr-Choinière, O.; Laliberté, F.; Doiron-Leyraud, N.; Ramshaw, B.J.; Liang, R.; Bonn, D.A.; Hardy, W.N.; Taillefer, L. Broken rotational symmetry in the pseudogap phase of a high-T_c superconductor. *Nature* **2010**, *463*, 519–522.
143. Fradkin, E.; Kivelson, S.A.; Lawler, M.J.; Eisenstein, J.P.; Mackenzie, A.P. Nematic Fermi fluids in condensed matter physics. *Annu. Rev. Condens. Matter Phys.* **2010**, *1*, 153–178.
144. Fradkin, E.; Kivelson, S.A. Electron nematic phases proliferate. *Science* **2010**, *327*, 155–156.
145. Nagaev, E.L. Ferromagnetic domains in a semiconducting antiferromagnet. *Zh. Éksp. Teor. Fiz.* **1968**, *54*, 228–238.

146. Krivoglaz, M.A. Electron states near the phase transition point and in disordered systems. *Fiz. Tverd. Tela* **1969**, *11*, 2230–2240.
147. Krivoglaz, M.A.; Karasevskii, A.I. Condensation in in the system of polarons or fluctuons with the formation of the nonhomogeneous state and peculiarities of conductance. *Pis'ma Zh. Éksp. Teor. Fiz.* **1974**, *19*, 454–457.
148. Emery, V.J.; Kivelson, S.A. Frustrated electronic phase separation and high-temperature superconductors. *Physica C* **1993**, *209*, 597–621.
149. Emery, V.J.; Kivelson, S.A.; Tranquada, J.M. Stripe phases in high-temperature superconductors. *Proc. Natl. Acad. Sci. USA* **1999**, *96*, 8814–8817.
150. Carlson, E.W.; Emery, V.J.; Kivelson, S.A.; Orgad, D. Concepts in high temperature superconductivity. In *Superconductivity. Vol. 2: Novel Superconductors*; Bennemann, K.H., Ketterson, J.B., Eds.; Springer Verlag: Berlin, Germany, 2008; pp. 1225–1348.
151. Chakravarty, S. Quantum oscillations and key theoretical issues in high temperature superconductors from the perspective of density waves. *Rep. Prog. Phys.* **2011**, *74*, 022501.
152. Halperin, B.I.; Rice, T.M. The excitonic state at the semiconductor-semimetal transition. *Solid State Phys.* **1968**, *21*, 115–192.
153. Hanaguri, T.; Lupien, C.; Kohsaka, Y.; Lee, D.-H.; Azuma, M.; Takano, M.; Takagi, H.; Davis, J.C. A "checkerboard" electronic crystal state in lightly hole-doped $Ca_{2-x}Na_xCuO_2Cl_2$. *Nature* **2004**, *430*, 1001–1005.
154. Shen, K.M.; Ronning, F.; Lu, D.H.; Baumberger, F.; Ingle, N.J.C.; Lee, W.S.; Meevasana, W.; Kohsaka, Y.; Azuma, M.; Takano, M.; Takagi, H.; Shen, Z.-X. Nodal quasiparticles and antinodal charge ordering in $Ca_{2-x}Na_xCuO_2Cl_2$. *Science* **2005**, *307*, 901–904.
155. Hoffman, J.E.; Hudson, E.W.; Lang, K.M.; Madhavan, V.; Eisaki, H.; Uchida, S.; Davis, J.C. A four unit cell periodic pattern of quasi-particle states surrounding vortex cores in $Bi_2Sr_2CaCu_2O_{8+\delta}$. *Science* **2002**, *295*, 466–469.
156. Hoffman, J.E.; McElroy, K.; Lee, D.-H.; Lang, K.M.; Eisaki, H.; Uchida, S.; Davis, J.C. Imaging quasiparticle interference in $Bi_2Sr_2CaCu_2O_{8+\delta}$. *Science* **2002**, *297*, 1148–1151.
157. Vershinin, M.; Misra, S.; Ono, S.; Ando, Y.A.Y.; Yazdani, A. Local ordering in the pseudogap state of the high-T_c superconductor $Bi_2Sr_2CaCu_2O_{8+\delta}$. *Science* **2004**, *303*, 1995–1998.
158. Fang, A.; Howald, C.; Kaneko, N.; Greven, M.; Kapitulnik, A. Periodic coherence-peak height modulations in superconducting $Bi_2Sr_2CaCu_2O_{8+\delta}$. *Phys. Rev. B* **2004**, *70*, 214514.
159. Hashimoto, A.; Momono, N.; Oda, M.; Ido, M. Scanning tunneling microscopy and spectroscopy study of 4a x 4a electronic charge order and the inhomogeneous pairing gap in superconducting $Bi_2Sr_2CaCu_2O_{8+\delta}$. *Phys. Rev. B* **2006**, *74*, 064508.
160. Ma, J.-H.; Pan, Z.-H.; Niestemski, F.C.; Neupane, M.; Xu, Y.-M.; Richard, P.; Nakayama, K.; Sato, T.; Takahashi, T.; Luo, H.-Q.; Fang, L.; Wen, H.-H.; Wang, Z.; Ding, H.; Madhavan, V. Coexistence of competing orders with two energy gaps in real and momentum space in the high temperature superconductor $Bi_2Sr_{2-x}La_xCuO_{6+\delta}$. *Phys. Rev. Lett.* **2008**, *101*, 207002.
161. Fink, J.; Schierle, E.; Weschke, E.; Geck, J.; Hawthorn, D.; Soltwisch, V.; Wadati, H.; Wu, H.-H.; Dürr, H.A.; Wizent, N.; Büchner, B.; Sawatzky, G.A. Charge ordering in $La_{1.8-x}Eu_{0.2}Sr_xCuO4$ studied by resonant soft x-ray diffraction. *Phys. Rev. B* **2009**, *79*, 100502.

162. Fink, J.; Soltwisch, V.; Geck, J.; Schierle, E.; Weschke, E.; Büchner, B. Phase diagram of charge order in $La_{1.8-x}Eu_{0.2}Sr_xCuO_4$ from resonant soft x-ray diffraction. *Phys. Rev. B* **2011**, *83*, 092503.
163. Li, X.M.; Li, F.H.; Luo, H.Q.; Fang, L.; Wen, H.-H. Transmission electron microscopy study of one-dimensional incommensurate structural modulation in superconducting oxides $Bi_{2+x}Sr_{2-x}CuO_{6+\delta}$ ($0.10 \leq x \leq 0.40$). *Supercond. Sci. Technol.* **2009**, *22*, 065003.
164. Sugimoto, A.; Kashiwaya, S.; Eisaki, H.; Yamaguchi, H.; Oka, K.; Kashiwaya, H.; Tsuchiura, H.; Tanaka, Y. Correlation between modulation structure and electronic inhomogeneity on Pb-doped Bi-2212 single crystals. *Physica C* **2005**, *426–431*, 390–395.
165. Bianconi, A.; Lusignoli, M.; Saini, N.L.; Bordet, P.; Kvick, A.; Radaelli, P.G. Stripe structure of the CuO_2 plane in $Bi_2Sr_2CaCu_2O_{8+y}$ by anomalous x-ray diffraction. *Phys. Rev. B* **1996**, *54*, 4310–4314.
166. Castellan, J.P.; Gaulin, B.D.; Dabkowska, H.A.; Nabialek, A.; Gu, G.; Liu, X.; Islam, Z. Two- and three-dimensional incommensurate modulation in optimally-doped $Bi_2Sr_2CaCu_2O_{8+\delta}$. *Phys. Rev. B* **2006**, *73*, 174505.
167. LeBoeuf, D.; Doiron-Leyraud, N.; Vignolle, B.; Sutherland, M.; Ramshaw, B.J.; Levallois, J.; Daou, R.; Laliberté, F.; Cyr-Choinière, O.; Chang, J.; Jo, Y.J.; Balicas, L.; Liang, R.; Bonn, D.A.; Hardy, W.N.; Proust, C.; Taillefer, L. Lifshitz critical point in the cuprate superconductor $YBa_2Cu_3O_y$ from high-field Hall effect measurements. *Phys. Rev. B* **2011**, *83*, 054506.
168. Vojta, M. Picking the cuprates' Fermi pockets. *Physics* **2011**, *4*, doi: 10.1103/Physics.4.12.
169. Uchida, M.; Ishizaka, K.; Hansmann, P.; Kaneko, Y.; Ishida, Y.; Yang, X.; Kumai, R.; Toschi, A.; Onose, Y.; Arita, R.; *et al.* Pseudogap of metallic layered nickelate $R_{2-x}Sr_xNiO_4$ (R = Nd, Eu) crystals measured using angle-resolved photoemission spectroscopy. *Phys. Rev. Lett.* **2011**, *106*, 027001.
170. Wilson, J.A.; Di Salvo, F.J.; Mahajan, S. Charge-density waves and superlattices in the metallic layered transition metal dichalcogenides. *Adv. Phys.* **1975**, *24*, 117–201.
171. Borisenko, S.V.; Kordyuk, A.A.; Yaresko, A.; Zabolotnyy, V.B.; Inosov, D.S.; Schuster, R.; Büchner, B.; Weber, R.; Follath, R.; Patthey, L.; Berger, H. Pseudogap and charge density waves in two dimensions. *Phys. Rev. Lett.* **2008**, *100*, 196402.
172. Inosov, D.S.; Zabolotnyy, V.B.; Evtushinsky, D.V.; Kordyuk, A.A.; Büchner, B.; Follath, R.; Berger, H.; Borisenko, S.V. Fermi surface nesting in several transition metal dichalcogenides. *New J. Phys.* **2008**, *10*, 125027.
173. Borisenko, S.V.; Kordyuk, A.A.; Zabolotnyy, V.B.; Inosov, D.S.; Evtushinsky, D.; Büchner, B.; Yaresko, A.N.; Varykhalov, A.; Follath, R.; Eberhardt, W.; Patthey, L.; Berger, H. Two energy gaps and Fermi-surface "arcs" in $NbSe_2$. *Phys. Rev. Lett.* **2009**, *102*, 166402.
174. Inosov, D.S.; Evtushinsky, D.V.; Zabolotnyy, V.B.; Kordyuk, A.A.; Büchner, B.; Follath, R.; Berger, H.; Borisenko, S.V. Temperature-dependent Fermi surface of $2H$-$TaSe_2$ driven by competing density wave order fluctuations. *Phys. Rev. B* **2009**, *79*, 125112.
175. Klemm, R.A. Striking similarities between the pseudogap phenomena in cuprates and in layered organic and dichalcogenide superconductors. *Physica C* **2000**, *341–348*, 839–842.

176. Lee, P.A.; Rice, T.M.; Anderson, P.W. Fluctuation effects at a Peierls transition. *Phys. Rev. Lett.* **1973**, *31*, 462–465.
177. Bulaevskii, L.N. Structural (Peierls) transition in quasi-one-dimensional crystals. *Usp. Fiz. Nauk* **1975**, *115*, 263–300.
178. Brazovskii, S.A.; Matveenko, S.I. Pseudogaps in incommensurate charge density waves and one-dimensional semiconductors. *Zh. Éksp. Teor. Fiz.* **2003**, *123*, 625–634.
179. Gabovich, A.M.; Medvedev, V.A.; Moiseev, D.P.; Motuz, A.A.; Prikhot'ko, A.F.; Prokopovich, L.V.; Solodukhin, A.V.; Khirunenko, L.I.; Shinkarenko, V.K.; Shpigel, A.S.; Yachmenev, V.E. Superconductivity and temperature anomalies of crystal lattice properties for metaloxide $La_{1.8}Ba_{0.2}CuO_{4-y}$. *Fiz. Nizk. Temp.* **1987**, *13*, 844–847.
180. Gabovich, A.M. Partial Dielectrization Model for Oxide Superconductivity. In *High-T_c Superconductivity, Experiment and Theory*; Davydov, A.S., Loktev, V.M., Eds.; Springer Verlag: Berlin, Germany, 1992; pp. 161–169.
181. Eremin, I.; Eremin, M. CDW as a possible reason for the pseudogap in the normal state of high-T_c cuprates. *J. Supercond.* **1997**, *10*, 459–460.
182. Ekino, T.; Sezaki, Y.; Fujii, H. Features of the energy gap above T_c in $Bi_2Sr_2CaCu_2O_{8+\delta}$ as seen by break-junction tunneling. *Phys. Rev. B* **1999**, *60*, 6916–6922.
183. Demsar, J.; Hudej, R.; Karpinski, J.; Kabanov, V.V.; Mihailovic, D. Quasiparticle dynamics and gap structure in $HgBa_2Ca_2Cu_3O_{8+\delta}$ investigated with femtosecond spectroscopy. *Phys. Rev. B* **2001**, *63*, 054519.
184. Le Tacon, M.; Sacuto, A.; Georges, A.; Kotliar, G.; Gallais, Y.; Colson, D.; Forget, A. Two energy scales and two distinct quasiparticle dynamics in the superconducting state of underdoped cuprates. *Nat. Phys.* **2006**, *2*, 537–543.
185. Tanaka, K.; Lee, W.S.; Lu, D.H.; Fujimori, A.; Fujii, T.; Risdiana.; Terasaki, I.; Scalapino, D.J.; Devereaux, T.P.; Hussain, Z.; Shen, Z.-X. Distinct Fermi-momentum-dependent energy gaps in deeply underdoped Bi2212. *Science* **2006**, *314*, 1910–1913.
186. Das, T.; Markiewicz, R.S.; Bansil, A. Competing order scenario of two-gap behavior in hole-doped cuprates. *Phys. Rev. B* **2008**, *77*, 134516.
187. Lee, W.S.; Vishik, I.M.; Lu, D.H.; Shen, Z.-X. A brief update of angle-resolved photoemission spectroscopy on a correlated electron system. *J. Phys. Condens. Matter* **2009**, *21*, 164217.
188. Kordyuk, A.A.; Borisenko, S.V.; Zabolotnyy, V.B.; Schuster, R.; Inosov, D.S.; Evtushinsky, D.V.; Plyushchay, A.I.; Follath, R.; Varykhalov, A.; Patthey, L.; Berger, H. Nonmonotonic pseudogap in high-T_c cuprates. *Phys. Rev. B* **2009**, *79*, 020504.
189. Teague, M.L.; Beyer, A.D.; Grinolds, M.S.; Lee, S.I.; Yeh, N.-C. Observation of vortices and hidden pseudogap from scanning tunneling spectroscopic studies of the electron-doped cuprate superconductor $Sr_{0.9}La_{0.1}CuO_2$. *Europhys. Lett.* **2009**, *85*, 17004.
190. Seibold, G.; Grilli, M.; Lorenzana, J. Dynamics of electronic inhomogeneities in cuprates. *J. Supercond.* **2011**, *24*, 1177–1179.
191. Emery, V.J.; Kivelson, S.A. Importance of phase fluctuations in superconductors with small superfluid density. *Nature* **1995**, *374*, 434–437.

192. Norman, M.; Pines, D.; Kallin, C. The pseudogap: Friend or foe of high T_c? *Adv. Phys.* **2005**, *54*, 715–733.
193. Chen, Q.; Stajic, J.; Tan, S.; Levin, K. BCS-BEC crossover: From high temperature superconductors to ultracold superfluids. *Phys. Rep.* **2005**, *412*, 188.
194. Valla, T.; Fedorov, A.V.; Lee, J.; Davis, J.C.; Gu, G.D. The ground state of the pseudogap in cuprate superconductors. *Science* **2006**, *314*, 1914–1916.
195. Kanigel, A.; Chatterjee, U.; Randeria, M.; Norman, M.R.; Souma, S.; Shi, M.; Li, Z.Z.; Raffy, H.; Campuzano, J.C. Protected nodes and the collapse of Fermi arcs in high-T_c cuprate superconductors. *Phys. Rev. Lett.* **2007**, *99*, 157001.
196. Kanigel, A.; Chatterjee, U.; Randeria, M.; Norman, M.R.; Koren, G.; Kadowaki, K.; Campuzano, J.C. Evidence for pairing above the transition temperature of cuprate superconductors from the electronic dispersion in the pseudogap phase. *Phys. Rev. Lett.* **2008**, *101*, 137002.
197. Yang, H.-B.; Rameau, J.D.; Johnson, P.D.; Valla, T.; Tsvelik, A.; Gu, G.D. Emergence of preformed Cooper pairs from the doped Mott insulating state in $Bi_2Sr_2CaCu_2O_{8+\delta}$. *Nature* **2008**, *456*, 77–80.
198. Shi, M.; Chang, J.; Pailhés, S.; Norman, M.R.; Campuzano, J.C.; Månsson, M.; Claesson, T.; Tjernberg, O.; Bendounan, A.; Patthey, L.; Momono, N.; Oda, M.; Ido, M.; Mudry, C.; Mesot, J. Coherent *d*-wave superconducting gap in underdoped $La_{2-x}Sr_xCuO_4$ by angle-resolved photoemission spectroscopy. *Phys. Rev. Lett.* **2008**, *101*, 047002.
199. Hüfner, S.; Müller, F. Temperature dependence of the gaps of high-temperature superconductors in the Fermi-arc region. *Phys. Rev. B* **2008**, *78*, 014521.
200. Hüfner, S.; Hossain, M.A.; Damascelli, A.; Sawatzky, G.A. Two gaps make a high-temperature superconductor? *Rep. Prog. Phys.* **2008**, *71*, 062501.
201. Meng, J.; Zhang, W.; Liu, G.; Zhao, L.; Liu, H.; Jia, X.; Lu, W.; Dong, X.; Wang, G.; Zhang, H.; *et al.* Monotonic d-wave superconducting gap of the optimally doped $Bi_2Sr_{1.6}La_{0.4}CuO_6$ superconductor by laser-based angle-resolved photoemission spectroscopy. *Phys. Rev. B* **2009**, *79*, 024514.
202. Krasnov, V.M. Interlayer tunneling spectroscopy of $Bi_2Sr_2CaCu_2O_{8+\delta}$: a look from inside on the doping phase diagram of high T_c superconductors. *Phys. Rev. B* **2002**, *65*, 140504.
203. Chia, E.E.M.; Zhu, J.-X.; Talbayev, D.; Averitt, R.D.; Taylor, A.J.; Oh, K.-H.; Jo, I.-S.; Lee, S.-I. Observation of competing order in a high-T_c superconductor using femtosecond optical pulses. *Phys. Rev. Lett.* **2007**, *99*, 147008.
204. Tanaka, K.; Lee, W.S.; Hussain, Z.; Shen, Z.X. Direct evidence of two gaps in underdoped Bi2212. *J. Phys. Conf. Ser.* **2008**, *108*, 012014.
205. Kondo, T.; Khasanov, R.; Takeuchi, T.; Schmalian, J.; Kaminski, A. Competition between the pseudogap and superconductivity in the high-T_c copper oxides. *Nature* **2009**, *457*, 296–300.
206. Hashimoto, M.; Yoshida, T.; Fujimori, A.; Li, D.H.; Shen, Z.-X.; Kubota, M.; Ono, K.; Ishikado, M.; Fujita, K.; Uchida, S. Effects of out-of-plane disorder on the nodal quasiparticle and superconducting gap in single-layer $Bi_2Sr_{1.6}L_{0.4}CuO_{6+\delta}$ (L = La,Nd,Gd). *Phys. Rev. B* **2009**, *79*, 144517.

207. Krasnov, V.M.; Kovalev, A.E.; Yurgens, A.; Winkler, D. Magnetic field dependence of the superconducting gap and the pseudogap in Bi2212 and $HgBr_2$-Bi2212, studied by intrinsic tunneling spectroscopy. *Phys. Rev. Lett.* **2001**, *86*, 2657–2660.
208. Bondar', A.V.; Ryabchenko, S.M.; Fedotov, Yu.V.; Motuz, A.A. Temperature dependence anomalies of nuclear relaxation for nuclei ^{63}Cu in $YBa_2Cu_3O_{7-x}$. *Pis'ma Zh. Éksp. Teor. Fiz.* **1989**, *50*, 133–134.
209. Krämer, S.; Mehring, M. Low-temperature charge ordering in the superconducting state of $YBa_2Cu_3O_{7-\delta}$. *Phys. Rev. Lett.* **1999**, *83*, 396–399.
210. Moncton, D.E.; Axe, J.D.; DiSalvo, F.J. Neutron scattering study of charge-density wave transitions in $2H$-$TaSe_2$ and $2H$-$NbSe_2$. *Phys. Rev. B* **1977**, *16*, 801–819.
211. He, R.-H.; Tanaka, K.; Mo, S.-K.; Sasagawa, T.; Fujita, M.; Adachi, T.; Mannella, N.; Yamada, K.; Koike, Y.; Hussain, Z.; Shen, Z.-H. Energy gaps in the failed high-T_c superconductor $La_{1.875}Ba_{0.125}CuO_4$. *Nat. Phys.* **2009**, *5*, 119–123.
212. Okada, Y.; Kawaguchi, T.; Ohkawa, M.; Ishizaka, K.; Takeuchi, T.; Shin, S.; Ikuta, H. Three energy scales characterizing the competing pseudogap state, the incoherent, and the coherent superconducting state in high-T_c cuprates. *Phys. Rev. B* **2011**, *83*, 104502.
213. Machida, K. Spin density wave and superconductivity in highly anisotropic materials. *J. Phys. Soc. Jpn.* **1981**, *50*, 2195–2202.
214. Machida, K.; Matsubara, T. Spin density wave and superconductivity in highly anisotropic materials. II. Detailed study of phase transitions. *J. Phys. Soc. Jpn.* **1981**, *50*, 3231–3239.
215. Machida, K. Spin density wave and superconductivity in highly anisotropic materials. III. Energy gap structure and non-magnetic impurity effects. *J. Phys. Soc. Jpn.* **1982**, *51*, 1420–1427.
216. Gabovich, A.M.; Moiseev, D.P. Metalloxide superconductor $BaPb_{1-x}Bi_xO_3$: Unusual properties and new applications. *Usp. Fiz. Nauk* **1986**, *150*, 599–623.
217. Ishida, Y.; Shimojima, T.; Ishizaka, K.; Kiss, T.; Okawa, M.; Togashi, T.; Watanabe, S.; Wang, X.-Y.; Chen, C.-T.; Kamihara, Y.; Hirano, M.; Hosono, H.; Shin, S. Temperature-dependent pseudogap in the oxypnictides $LaFeAsO_{1-x}F_x$ and $LaFePO_{1-x}F_x$ seen via angle-integrated photoemission. *Phys. Rev. B* **2009**, *79*, 060503.
218. Mertelj, T.; Kabanov, V.V.; Gadermaier, C.; Zhigadlo, N.D.; Katrych, S.; Karpinski, J.; Mihailovic, D. Distinct pseudogap and quasiparticle relaxation dynamics in the superconducting state of nearly optimally doped $SmFeAsO_{0.8}F_{0.2}$ single crystals. *Phys. Rev. Lett.* **2009**, *102*, 117002.
219. Zabolotnyy, V.B.; Inosov, D.S.; Evtushinsky, D.V.; Koitzsch, A.; Kordyuk, A.A.; Sun, G.L.; Park, J.T.; Haug, D.; Hinkov, V.; Boris, A.V.; *et al.* (π, π) electronic order in iron arsenide superconductors. *Nature* **2009**, *457*, 569–572.
220. Littlewood, P.B.; Heine, V. The effect of electron-electron interactions on the Peierls transition in metals with strong nesting of Fermi surfaces. *J. Phys. C* **1981**, *14*, 2943–2949.
221. Mazin, I.I.; Schmalian, J. Pairing symmetry and pairing state in ferropnictides: Theoretical overview. *Physica C* **2009**, *469*, 614–627.
222. Rotter, M.; Tegel, M.; Johrendt, D.; Schellenberg, I.; Hermes, W.; Pöttgen, R. Spin-density-wave anomaly at 140 K in the ternary iron arsenide $BaFe_2As_2$. *Phys. Rev. B* **2008**, *78*, 020503.

223. Pickett, W.E. Electronic structure of the high-temperature oxide superconductors. *Rev. Mod. Phys.* **1989**, *61*, 433–512, doi:10.1103/RevModPhys.61.433.
224. Volkov, B.A. Structural and magnetic transformations in narrow-gap semiconductors and semimetals. *Trudy Fiz. Inst. Akad. Nauk SSSR* **1978**, *104*, 3–57.
225. Littlewood, P.B. Collective modes and superconductivity in an extended Hubbard model for copper oxide superconductors. *Phys. Rev. B* **1990**, *42*, 10075–10089.
226. Grüner, G. *Density Waves in Solids*; Addison-Wesley Publishing Company: Reading, MA, USA, 1994; p. 259.
227. van Wezel, J.; Nahai-Williamson, P.; Saxena, S.S. Exciton-phonon interactions and superconductivity bordering charge order in $TiSe_2$. *Phys. Rev. B* **2011**, *83*, 024502.
228. Morosan, E.; Zandbergen, H.W.; Dennis, B.S.; Bos, J.W.G.; Onose, Y.; Klimczuk, T.; Ramirez, A.P.; Ong, N.P.; Cava, R.J. Superconductivity in Cu_xTiSe_2. *Nat. Phys.* **2006**, *2*, 544–550.
229. Kusmartseva, A.F.; Sipos, B.; Berger, H.; Forró, L.; Tutiš, E. Pressure induced superconductivity in pristine $1T$-$TiSe_2$. *Phys. Rev. Lett.* **2009**, *103*, 236401.
230. Won, H.; Maki, K. d-wave superconductor as a model of high-T_c superconductors. *Phys. Rev. B* **1994**, *49*, 1397–1402.
231. Maki, K.; Won, H. Why d-wave superconductivity? *J. Phys. I (Paris)* **1996**, *6*, 2317–2326.
232. Pickett, W.E.; Krakauer, H.; Cohen, R.E.; Singh, D.J. Fermi surfaces, Fermi liquids, and high-temperature superconductors. *Science* **1992**, *255*, 46–54.
233. Markiewicz, R.S.; Sahrakorpi, S.; Lindroos, M.; Lin, H.; Bansil, A. One-band tight-binding model parametrization of the high-T_c cuprates including the effect of k_z dispersion. *Phys. Rev. B* **2005**, *72*, 054519.
234. Abrikosov, A.A.; Gor'kov, L.P.; Dzyaloshinskii, I.E. *Methods of Quantum Field Theory in Statistical Physics*; Prentice Hall: Englewood Cliffs, NJ, USA, 1963.
235. Mühlschlegel, B. Die thermodynamischen Funktionen des Supraleiters. *Z. Phys.* **1959**, *155*, 313–327.
236. Loram, J.W.; Mirza, K.A.; Cooper, J.R.; Tallon, J.L. Superconducting and normal state energy gaps in $Y_{0.8}Ca_{0.2}Ba_2Cu_3O_{7-\delta}$ from the elctronic specific heat. *Physica C* **1997**, *282–287*, 1405–1406.
237. Williams, G.V.M.; Tallon, J.L.; Haines, E.M.; Michalak, R.; Dupree, R. NMR evidence for a d-wave normal-state pseudogap. *Phys. Rev. Lett.* **1997**, *78*, 721–724.
238. Trunin, M.R.; Nefyodov, Yu.A.; Shevchun, A.F. Superfluid density in the underdoped $YBa_2Cu_3O_{7-x}$: Evidence for *d*-density-wave order of the pseudogap. *Phys. Rev. Lett.* **2004**, *92*, 067006.
239. Kurosawa, T.; Yoneyama, T.; Takano, Y.; Hagiwara, M.; Inoue, R.; Hagiwara, N.; Kurusu, K.; Takeyama, K.; Momono, N.; Oda, M.; Ido, M. Large pseudogap and nodal superconducting gap in $Bi_2Sr_{2-x}La_xCuO_{6+\delta}$ and $Bi_2Sr_2CaCu_2O_{8+\delta}$: Scanning tunneling microscopy and spectroscopy. *Phys. Rev. B* **2010**, *81*, 094519.
240. Dahm, T.; Manske, D.; Tewordt, L. Charge-density-wave and superconductivity d-wave gaps in the Hubbard model for underdoped high-T_c cuprates. *Phys. Rev. B* **1997**, *56*, 11419–11422.

241. Kim, W.; Zhu, J.-X.; Carbotte, J.P.; Ting, C.S. c-axis response of a high-T_c superconductor with d-density-wave order. *Phys. Rev. B* **2002**, *65*, 064502.
242. Morr, D.K. A hidden order in the cuprate superconductors: The d-density-wave phase. *J. Supercond.* **2003**, *16*, 487–490.
243. Andersen, B.M. Two nonmagnetic impurities in the d-wave-superconducting and d-density-wave states of the cuprate superconductors as a probe for the pseudogap. *Phys. Rev. B* **2003**, *68*, 094518.
244. Oganesyan, V.; Ussishkin, I. Nernst effect, quasiparticles, and d-density waves in cuprates. *Phys. Rev. B* **2004**, *70*, 054503.
245. Andrenacci, N.; Angilella, G.G.N.; Beck, H.; Pucci, R. Linear response theory around a localized impurity in the pseudogap regime of an anisotropic superconductor: Precursor pairing versus d-density-wave scenario. *Phys. Rev. B* **2004**, *70*, 024507.
246. Ghosh, A. DDW Order and Its Role in Cuprates. In *Progress in Superconductivity Research*; Chang, O.A., Ed.; Nova Science: New York, NY, USA, 2008; pp. 123–162.
247. Zhang, C.; Tewari, S.; Chakravarty, S. Quasiparticle Nernst effect in the cuprate superconductors from the d-density-wave theory of the pseudogap phase. *Phys. Rev. B* **2010**, *81*, 104517.
248. Ha, K.; Subok, R.; Ilmyong, R.; Cheongsong, K.; Yuling, F. Superconductivity enhanced by d-density wave: A weak-coupling theory. *Physica B* **2011**, *406*, 1459–1465.
249. Scalapino, D.J. The case for $d_{x^2-y^2}$ pairing in the cuprate superconductors. *Phys. Rep.* **1995**, *250*, 329–365.
250. Leggett, A.J. *Quantum Liquids: Bose Condensation and Cooper Pairing in Condensed-Matter Systems*; University Press: Oxford, UK, 2006; p. 388.
251. Pereg-Barnea, T.; Weber, H.; Refael, G.; Franz, M. Quantum oscillations from Fermi arcs. *Nat. Phys.* **2010**, *6*, 44–49.
252. Hoffman, J.E. To pair or not to pair? *Nat. Phys.* **2010**, *6*, 404–405.
253. Annett, J.F. *Superconductivity, Superfluids and Condensates*; University Press: Oxford, UK, 2004; p. 186.
254. Hackl, A.; Vojta, M.; Sachdev, S. Quasiparticle Nernst effect in stripe-ordered cuprates. *Phys. Rev. B* **2010**, *81*, 045102.
255. Yang, K.; Sondhi, S.L. Response of a $d_{x^2-y^2}$ superconductor to a Zeeman magnetic field. *Phys. Rev. B* **1998**, *57*, 8566–8570.
256. Jérome, D.; Berthier, C.; Molinié, P.; Rouxel, J. Electronic properties of transition metal dichalcogenides: Connection between structural instabilities and superconductivity. *J. Phys. (Paris) Colloq.* **1976**, *37*, C125–C135.
257. Bud'ko, S.L.; Canfield, P.C.; Morosan, E.; Cava, R.J.; Schmiedeshoff, G.M. Thermal expansion and effect of pressure on superconductivity in Cu_xTiSe_2. *J. Phys. Condens. Matter* **2007**, *19*, 176230.
258. Graf, D.; Brooks, J.S.; Almeida, M.; Dias, J.C.; Uji, S.; Terashima, T.; Kimata, M. Evolution of superconductivity from a charge-density-wave ground state in pressurized $(Per)_2[Au(mnt)_2]$. *Europhys. Lett.* **2009**, *85*, 27009.

259. Hamlin, J.J.; Zocco, D.A.; Sayles, T.A.; Maple, M.B.; Chu, J.-H.; Fisher, I.R. Pressure-induced superconducting phase in the charge-density-wave compound terbium tritelluride. *Phys. Rev. Lett.* **2009**, *102*, 177002.
260. Takeshita, N.; Sasagawa, T.; Sugioka, T.; Tokura, Y.; Takagi, H. Gigantic anisotropic uniaxial pressure effect on superconductivity within the CuO_2 plane of $La_{1.64}Eu_{0.2}Sr_{0.16}CuO_4$: Strain control of stripe criticality. *J. Phys. Soc. Jpn.* **2004**, *73*, 1123–1126.
261. Gabovich, A.M.; Voitenko, A.I. Influence of inelastic quasiparticle scattering on thermodynamic and transport properties of high-T_c oxides. *Physica C* **1996**, *258*, 236–252.
262. Manske, D. *Theory of Unconventional Superconductors. Cooper-Pairing Mediated by Spin Excitations*; Springer Verlag: New York, NY, USA, 2004; p. 228.
263. Abrikosov, A.A. *Fundamentals of the Theory of Metals*; North-Holland: Amsterdam, The Netherlands, 1988.
264. de Llano, M.; Annett, J.F. Generalized Cooper pairing in superconductors. *Int. J. Mod. Phys. B* **2007**, *21*, 3657–3686.
265. Kondepudi, D.; Prigogine, I. *Modern Thermodynamics. From Heat Engines to Dissipative Structures*; John Wiley and Sons: Chichister, UK, 1999.
266. Marsiglio, F.; Carbotte, J.P. Electron-Phonon Superconductivity. In *Superconductivity. Vol. 1: Conventional and Unconventional Superconductors*; Bennemann, K.H., Ketterson, J.B., Eds.; Springer Verlag: Berlin, Germany, 2008; pp. 73–162.
267. Hasegawa, T.; Ikuta, H.; Kitazawa, K. Tunneling Spectroscopy of Oxide Superconductors. In *Physical Properties of High Temperature Superconductors III*; Ginsberg, D.M., Ed.; World Scientific: Singapore, 1992; pp. 525–630.
268. Wei, J.Y.T.; Tsuei, C.C.; van Bentum, P.J.M.; Xiong, Q.; Chu, C.W.; Wu, M.K. Quasiparticle tunneling spectra of the high-T_c mercury cuprates: Implications of the *d*-wave two-dimensional van Hove scenario. *Phys. Rev. B* **1998**, *57*, 3650–3662.
269. Gomes, K.K.; Pasupathy, A.N.; Pushp, A.; Ono, S.; Ando, Y.; Yazdani, A. Visualizing pair formation on the atomic scale in the high-T_c superconductor $Bi_2Sr_2CaCu_2O_{8+\delta}$. *Nature* **2007**, *447*, 569–572.
270. Geilikman, B.T.; Kresin, V.Z.; Masharov, N.F. Transition temperature and energy gap for superconductors with strong coupling. *J. Low Temp. Phys.* **1975**, *18*, 241–271.
271. Carbotte, J.P.; Jiang, C. Strong-coupling effects in *d*-wave superconductors. *Phys. Rev. B* **1993**, *48*, 4231–4234.
272. Miyakawa, N.; Guptasarma, P.; Zasadzinski, J.F.; Hinks, D.G.; Gray, K.E. Strong dependence of the superconducting gap on oxygen doping from tunneling measurements on $Bi_2Sr_2CaCu_2O_{8+\delta}$. *Phys. Rev. Lett.* **1998**, *80*, 157–160.
273. Kulić, M.L. Interplay of electron-phonon interaction and strong correlations: The possible way to high-temperature superconductivity. *Phys. Rep.* **2000**, *338*, 1–264.
274. Izyumov, Yu.A.; Kurmaev, E.Z. Strongly electron-correlated materials. *Usp. Fiz. Nauk* **2008**, *178*, 25–60.
275. Alloul, H.; Bobroff, J.; Gabay, M.; Hirschfeld, P.J. Defects in correlated metals and superconductors. *Rev. Mod. Phys.* **2009**, *81*, 45–108.

276. Meng, J.-Q.; Brunner, M.; Kim, K.-H.; Lee, H.-G.; Lee, S.-I.; Wen, J.S.; Xu, Z.J.; Gu, G.D.; Gweon, G.-H. Momentum-space electronic structures and charge orders of the high-temperature superconductors $Ca_{2-x}Na_xCuO_2Cl_2$ and $Bi_2Sr_2CaCu_2O_{8+\delta}$. *Phys. Rev. B* **2011**, *84*, 060513.
277. Schuster, H.G. Influence of dilute nonmagnetic impurities on the Peierls instability in one-dimensional conductors. *Solid State Commun.* **1974**, *14*, 127–129.
278. Zittartz, J. Theory of the excitonic insulator in the presence of normal impurities. *Phys. Rev.* **1967**, *164*, 575–582.
279. Whangbo, M.H.; Canadell, E.; Foury, P.; Pouget, J.P. Hidden Fermi surface nesting and charge density wave instability in low-dimensional metals. *Science* **1991**, *252*, 96–98.
280. Johannes, M.D.; Mazin, I.I. Fermi surface nesting and the origin of charge density waves in metals. *Phys. Rev. B* **2008**, *77*, 165135.
281. Raymond, S.; Bouchet, J.; Lander, G.H.; Le Tacon, M.; Garbarino, G.; Hoesch, M.; Rueff, J.-P.; Krisch, M.; Lashley, J.C.; Schulze, R.K.; Albers, R.C. Understanding the complex phase diagram of Uranium: The role of electron-phonon coupling. *Phys. Rev. Lett.* **2011**, *107*, 136401.
282. Weber, F.; Rosenkranz, S.; Castellan, J.-P.; Osborn, R.; Hott, R.; Heid, R.; Bohnen, K.-P.; Egami, T.; Said, A.H.; Reznik, D. Extended phonon collapse and the origin of the charge-density wave in $2H$-$NbSe_2$. *Phys. Rev. Lett.* **2011**, *107*, 107403.
283. Vedeneev, S.I.; Piot, B.A.; Maude, D.K. Magnetic field dependence of the superconducting energy gap in $Bi_2Sr_2CaCu_2O_{8+\delta}$ probed using break-junction tunneling spectroscopy. *Phys. Rev. B* **2010**, *81*, 054501.
284. Lubashevsky, Y.; Garg, A.; Sassa, Y.; Shi, M.; Kanigel, A. Insensitivity of the superconducting gap to variations in the critical temperature of Zn-substituted $Bi_2Sr_2CaCu_2O_{8+\delta}$ superconductors. *Phys. Rev. Lett.* **2011**, *106*, 047002.
285. Anderson, P.W. *The Theory of Superconductivity in the High-T_c Cuprates*; Princeton Univeristy Press: Princeton, NJ, USA, 1997; p. 446.
286. Anderson, P.W.; Lee, P.A.; Randeria, M.; Rice, T.M.; Trivedi, N.; Zhang, F.C. The physics behind high-temperature superconducting cuprates: The "plain vanilla" version of RVB. *J. Phys. Condens. Matter* **2004**, *16*, R755–R769.
287. Alexandrov, A.S. High-temperature superconductivity: The explanation. *Phys. Scr.* **2011**, *83*, 038301.
288. Anderson, P.W. BCS: The scientific "love of my life". *Int. J. Mod. Phys. B* **2010**, *24*, 3983–3998.
289. Zhao, G.M. The pairing mechanism of high-temperature superconductivity: Experimental constraints. *Phys. Scr.* **2011**, *83*, 038302.
290. Plakida, N.M. Comment on "The pairing mechanism of high-temperature superconductivity: Experimental constraints". *Phys. Scr.* **2011**, *83*, 038303.
291. Zhao, G.M. Reply to Comment on "The pairing mechanism of high-temperature superconductivity: Experimental constraints". *Phys. Scr.* **2011**, *83*, 038304.
292. Anderson, P.W. Personal history of my engagement with cuprate superconductivity, 1986–2010. *Int. J. Mod. Phys. B* **2011**, *25*, 1–39.
293. Alexandrov, A.S.; Kabanov, V.V. Unconventional high-temperature superconductivity from repulsive interactions: Theoretical constraints. *Phys. Rev. Lett.* **2011**, *106*, 136403.

294. Basov, D.N.; Chubukov, A.V. Manifesto for a higher T_c. *Nat. Phys.* **2011**, *7*, 272–276.
295. Norman, M.R. The challenge of unconventional superconductivity. *Science* **2011**, *332*, 196–200.
296. Ginzburg, V.L. Superconductivity: The day before yesterday, yesterday, today, to-morrow. *Usp. Fiz. Nauk* **2000**, *170*, 619–630.
297. Schmalian, J. Failed theories of superconductivity. *Mod. Phys. Lett. B* **2010**, *24*, 2679–2691.
298. Mazin, I. Iron superconductivity weathers another storm. *Physics* **2011**, *4*, 26.